NASA TECHNICAL NOTE

NASA TN D-6541

C.1

NASA TN D-6541

ANALYTICAL SOLUTION FOR THE WIND-DRIVEN CIRCULATION IN A LAKE CONTAINING AN ISLAND

by Marvin E. Goldstein and Richard T. Gedney

Lewis Research Center
Cleveland, Ohio 44135

NATIONAL AERONAUTICS AND SPACE ADMINISTRATION • WASHINGTON, D. C. • NOVEMBER 1971

1. Report No.	2. Government Accession No.	3. Recipient's Catalog No.
NASA TN D-6541		

4. Title and Subtitle	5. Report Date
ANALYTICAL SOLUTION FOR THE WIND-DRIVEN CIRCULATION IN A LAKE CONTAINING AN ISLAND	November 1971
	6. Performing Organization Code
7. Author(s)	8. Performing Organization Report No.
Marvin E. Goldstein and Richard T. Gedney	E-6335
	10. Work Unit No.
9. Performing Organization Name and Address	129-01
Lewis Research Center National Aeronautics and Space Administration Cleveland, Ohio 44135	11. Contract or Grant No.
	13. Type of Report and Period Covered
12. Sponsoring Agency Name and Address	Technical Note
National Aeronautics and Space Administration Washington, D.C. 20546	14. Sponsoring Agency Code

15. Supplementary Notes

16. Abstract

An analysis has been carried out to determine analytically the effect of an island on the wind driven currents in a shallow lake (or sea). A general analysis is developed that can be applied to a large class of lake and island geometries and bottom topographies. Detailed numerical results are obtained for a circular island located eccentrically or concentrically in a circular lake with a logarithmic bottom topography. It is shown that an island can produce volume flow (vertically integrated velocities) gyres that are completely different from those produced by a normal basin without an island. These gyres in the neighborhood of the island will produce different velocity patterns, which include the acceleration of flow near the island shore.

17. Key Words (Suggested by Author(s))	18. Distribution Statement
Three-dimensional turbulent flow Shallow-lake currents	Unclassified - unlimited

19. Security Classif. (of this report)	20. Security Classif. (of this page)	21. No. of Pages	22. Price*
Unclassified	Unclassified	78	$3.00

* For sale by the National Technical Information Service, Springfield, Virginia 22151

ANALYTICAL SOLUTION FOR THE WIND-DRIVEN CIRCULATION IN A LAKE CONTAINING AN ISLAND

by Marvin E. Goldstein and Richard T. Gedney
Lewis Research Center

SUMMARY

An analysis has been carried out to determine analytically the effect of an island on the wind driven currents in a shallow lake (or sea). A general analysis is developed that can be applied to a large class of lake and island geometries and bottom topographies. Detailed numerical results are obtained for a circular island located eccentrically or concentrically in a circular lake with a logarithmic bottom topography. It is shown that an island can produce volume flow (vertically integrated velocities) gyres that are completely different from those produced by a normal basin without an island. These gyres in the neighborhood of the island will produce different velocity patterns, which include the acceleration of flow near the island shore.

INTRODUCTION

Lake currents are very important in determining what chemical and biological changes will take place in a lake since they control the distributions of sediment and pollution which have been introduced. It is, therefore, important to be able to predict these currents.

The main source of motion in the oceans and lakes are the winds. When the winds act on the surface of a deep body of water, they set up a circulation which consists of a top and bottom Ekman (boundary) layer separated by a geostrophic (inviscid) core. For lakes, in which the depth is much greater than the thickness of the friction or Ekman layers, the usual Ekman dynamics (i. e., the bottom stress assumed proportional to be the geostrophic velocity) can be used. For any of the Great Lakes, the use of Ekman dynamics is questionable since they all have shallow shore regions of considerable extent. In Lake Erie, for moderate winds, the thickness of the Ekman layers are comparable to the depth over much of the lake and therefore the use of Ekman dynamics is not valid.

The necessary extension of the Ekman analysis to the case of a shallow lake has been given by Welander (ref. 1), and that theory has been used here. The solution for the surface displacement is first obtained. From this, the horizontal velocities are calculated as a function of depth and horizontal position in the lake. In the present analysis, only the motions caused by steady winds are considered. Gedney (ref. 2) has numerically calculated the velocities for Lake Erie using Welander's shallow sea formulation. Comparison of these calculations with measurements in Lake Erie show that steady-state currents actually do occur.

Goldstein, Braun, and Gedney (ref. 3) developed a method for obtaining product solutions to a certain class of partial differential equations. This class of equations includes Welander's equation for the wind-driven circulation in shallow lakes for a large class of bottom topographies. The method was used to reduce the problem of finding solutions to Welander's equation for a closed body of water to the problem of solving an ordinary differential equation. To illustrate the method, the complete analytical solution for an elliptically shaped body of water with a particular choice of bottom topography when the depth is greater than one-half the Ekman friction depth was given. In this analysis the method developed in reference 3 is extended to include the case when an island is included.

Previously, islands have been analyzed numerically in total studies, which included effects such as irregular mainland boundaries that have masked the island effect. This analysis is being performed to determine just the local effect due to an island so that a fundamental understanding is obtained. To date no such island analyses have been performed for a shallow lake.

BASIC EQUATIONS

In the present analysis the basic approximations are that the water density is constant, the vertical eddy viscosity is independent of depth but dependent on wind velocity, the pressure is hydrostatic, and the lateral friction and nonlinear acceleration terms can be neglected. The horizontal scale used to justify neglecting horizontal friction and nonlinear acceleration is of the order of the width of the lake. For regions close to the shore, usually of the order of 1 kilometer, the horizontal friction and nonlinear acceleration terms are important. Therefore, the lake must be much larger than 1 kilometer and the currents calculated herein are "large scale" currents that are valid in the interior region away from the shore areas.

These assumptions reduce the momentum equations to two equations containing as unknowns the horizontal velocities and the surface slope. The appropriate boundary conditions for these equations are a no-slip condition at the lake bottom and a specified shear stress (due to the wind) at the air-sea interface. These equations and boundary conditions can be solved analytically to give the velocity as a function of depth with the surface wind stress and surface slope as parameters.

By vertically integrating the momentum equations and by using the vertically integrated continuity equation, one can obtain a single equation for the surface displacement:

$$\zeta_{xx} + \zeta_{yy} + \left[A\left(2\pi \frac{h}{d}\right)_x - B\left(2\pi \frac{h}{d}\right)_y\right]\zeta_x + \left[A\left(2\pi \frac{h}{d}\right)_y + B\left(2\pi \frac{h}{d}\right)_x\right]\zeta_y = f \tag{1}$$

where ζ is the surface displacement of the sea or lake, h is the depth of the lake, x and y are the horizontal, locally Cartesian coordinates, $d\left(= \pi\sqrt{2\nu/f_c}\right)$ is the Ekman friction depth, ν is the coefficient of vertical eddy diffusivity, and f_c is the Coriolis parameter, which introduces the effect of the Earth's rotation. In addition,

$$\left.\begin{aligned} A &\equiv \frac{2\sin\left(2\pi \frac{h}{d}\right)\sinh\left(2\pi \frac{h}{d}\right)}{\left[\cosh\left(2\pi \frac{h}{d}\right) + \cos\left(2\pi \frac{h}{d}\right)\right]\left[\sinh\left(2\pi \frac{h}{d}\right) - \sin\left(2\pi \frac{h}{d}\right)\right]} \\ B &\equiv \frac{\sinh\left(2\pi \frac{h}{d}\right) + \sin\left(2\pi \frac{h}{d}\right)}{\cosh\left(2\pi \frac{h}{d}\right) + \cos\left(2\pi \frac{h}{d}\right)} \end{aligned}\right\} \tag{2}$$

$$f \equiv -\frac{1}{2\pi \frac{h}{d} E}\left[\sigma_x^{(1)} + \sigma_y^{(2)}\right] \tag{3}$$

where

$$\left.\begin{aligned} \sigma^{(1)} &\equiv \frac{2\pi\tau_1^w}{gd} C - \frac{2\pi\tau_2^w}{gd} D \\ \sigma^{(2)} &\equiv \frac{2\pi\tau_1^w}{gd} D + \frac{2\pi\tau_2^w}{gd} C \end{aligned}\right\} \tag{4}$$

$$\left.\begin{aligned} C &\equiv \frac{2\sin\left(\frac{\pi h}{d}\right)\sinh\left(\frac{\pi h}{d}\right)}{\cos\left(\frac{2\pi h}{d}\right)+\cosh\left(2\pi\frac{h}{d}\right)} \\ D &\equiv \frac{2\cos\left(\pi\frac{h}{d}\right)\cosh\left(\pi\frac{h}{d}\right)}{\cos\left(2\pi\frac{h}{d}\right)+\cosh\left(2\pi\frac{h}{d}\right)} - 1 \end{aligned}\right\} \tag{5}$$

$$E \equiv \frac{1}{\left(2\pi\frac{h}{d}\right)}\,\frac{\sin\left(2\pi\frac{h}{d}\right)-\sinh\left(2\pi\frac{h}{d}\right)}{\cos\left(2\pi\frac{h}{d}\right)+\cosh\left(2\pi\frac{h}{d}\right)} \tag{6}$$

where g is the acceleration due to gravity and τ_1^w and τ_2^w are, respectively, the x and y components of the wind stress divided by the density of water.

Equation (1) is a slightly rearranged form of that given by Welander (ref. 1). For details of the derivation of equation (6) and for a discussion of the approximations involved in the derivation, see Gedney (ref. 2). For instance, Gedney has shown for Lake Erie that the approximations used, except for the approximation of a constant eddy viscosity, induce at the most a small (of the order of 10^{-1}) or very local error in the calculations. It is shown in reference 3 that, when $h > \frac{1}{2}d$, the coefficients in this equation can be approximated quite closely by much simpler functions of h/d. Thus,

$$\left.\begin{aligned} A &\approx 0 \\ B &\approx 1 \end{aligned}\right\} \quad \text{for } \frac{h}{d} > \frac{1}{2} \tag{7}$$

$$f \approx \sigma_x^{(1)} + \sigma_y^{(2)} \qquad \text{for } \frac{h}{d} > \frac{1}{2} \tag{8}$$

$$\left.\begin{aligned} \sigma^{(1)} &\approx \frac{2\pi\tau_1^w}{gd}\,2e^{-\pi h/d}\sin\left(\pi\frac{h}{d}\right) + \frac{2\pi\tau_2^w}{gd}\left(1 - 2e^{-\pi h/d}\cos\left(\pi\frac{h}{d}\right)\right) \\ \sigma^{(2)} &\approx \frac{2\pi\tau_1^w}{gd}\left(2e^{-\pi h/d}\cos\left(\pi\frac{h}{d}\right) - 1\right) + \frac{2\pi\tau_2^w}{gd}\,2e^{-\pi h/d}\sin\left(\pi\frac{h}{d}\right) \end{aligned}\right\} \quad \text{for } \frac{h}{d} > \frac{1}{2} \tag{9}$$

The x and y components of the horizontal velocity U and V, respectively, can be found once the solution to equation (1) is known by using the relation (given in ref. 1)

$$(U + iV)\frac{f_c}{g} = \left[\frac{(1 - i)\pi\tau^W}{gd}\right]\frac{\sinh\left[(1 + i)\pi\left(\frac{h + \xi}{d}\right)\right]}{\cosh\left[(1 + i)\pi\frac{h}{d}\right]} - i\left\{\frac{\cosh\left[\pi(1 + i)\frac{\xi}{d}\right]}{\cosh\left[\pi(1 + i)\frac{h}{d}\right]} - 1\right\}\left(\frac{\partial\zeta}{\partial x} + i\frac{\partial\zeta}{\partial y}\right) \tag{10}$$

where ξ is the vertical distance below the water surface and where

$$\tau^W = \tau_1^W + i\tau_2^W \tag{11}$$

The x and y components of the total volume flow Q_1 and Q_2, respectively, can also be found from the surface displacement by using the relations

$$\left.\begin{aligned}\frac{Q_1 f_c}{gd} &\equiv \frac{f_c}{gd}\int_{-h}^{0} U\,d\xi = \frac{1}{2\pi}\left[\sigma^{(1)} + \frac{2\pi h}{d}(E\zeta_x - F\zeta_y)\right]\\ \frac{Q_2 f_c}{gd} &\equiv \frac{f_c}{gd}\int_{-h}^{0} V\,d\xi = \frac{1}{2\pi}\left[\sigma^{(2)} + \frac{2\pi h}{d}(F\zeta_x + E\zeta_y)\right]\end{aligned}\right\} \tag{12}$$

where

$$F \equiv -\frac{1}{2\pi\frac{h}{d}}\frac{\sin\left(2\pi\frac{h}{d}\right) + \sinh\left(2\pi\frac{h}{d}\right)}{\cos\left(2\pi\frac{h}{d}\right) + \cosh\left(2\pi\frac{h}{d}\right)} + 1 \tag{13}$$

When $h > \frac{1}{2}d$, equation (12) can be approximated closely by the simpler relation (ref. 3)

$$\frac{2\pi Q f_c}{gd} \approx \sigma - \left[(1 + i) - i\frac{2\pi h}{d}\right](\zeta_x + i\zeta_y) \qquad \text{for } \frac{h}{d} > \frac{1}{2} \tag{14}$$

where we have put

$$Q = Q_1 + iQ_2 \tag{15}$$

and

$$\sigma = \sigma^{(1)} + i\sigma^{(2)} \tag{16}$$

or, using equations (9) and (11) and collecting terms,

$$\sigma \approx i\,\frac{2\pi\tau^{W}}{gd}\left[2e^{-\pi(1+i)h/d} - 1\right] \qquad \text{for } \frac{h}{d} > \frac{1}{2} \tag{17}$$

The boundary conditions for equation (1) are obtained by specifying the normal volume flow at the coasts. Thus, if n_1 and n_2 are the x and y components, respectively, of the outward drawn unit normal $\hat{n}$ to the boundary, then for any closed body of water the boundary conditions for equation (1) are obtained by substituting equation (12) (or for the case where $(h/d) > (1/2)$ eq. (14)) into the relation

$$Q_1n_1 + Q_2n_2 = 0 \tag{18}$$

Class of Depth Distributions for Which Equations Can Be Solved

We shall now suppose that there exists a nonconstant harmonic function u of x and y and an arbitrary function H of u only such that the depth distribution h can be expressed in the form

$$\frac{h(x,y)}{d} = \frac{1}{2\pi}\,H[u(x,y)] \tag{19}$$

This is a fairly general functional form, and it will be possible, for any one of a large number of lakes and seas, to choose the functions u and H in equation (19) so that the depth distribution is approximated closely by a relation of this type.

When relation (19) is substituted into equations (1) and (2), we find that

$$\zeta_{xx} + \zeta_{yy} + 2\left[\alpha(u)u_x - \beta(u)u_y\right]\zeta_x + 2\left[\alpha(u)u_y + \beta(u)u_x\right]\zeta_y = f \tag{20}$$

where

$$\left.\begin{aligned}\alpha &\equiv -\frac{\sin H \sinh H}{(\cos H + \cosh H)(\sin H - \sinh H)}\frac{dH}{du}\\[2ex] \beta &\equiv \frac{1}{2}\frac{\sinh H + \sin H}{\cosh H + \cos H}\frac{dH}{du}\end{aligned}\right\} \tag{21}$$

$$f \equiv \frac{\cosh H + \cos H}{\sinh H - \sin H}\left[\frac{\partial \sigma^{(1)}}{\partial x} + \frac{\partial \sigma^{(2)}}{\partial y}\right] \tag{22}$$

or when $h > \frac{1}{2} d$ the coefficients α and β are given to a close approximation by

$$\left.\begin{aligned}\alpha &\approx 0\\[2ex] \beta &\approx \frac{1}{2}\frac{dH}{du}\end{aligned}\right\} \quad \text{for } \frac{h}{d} > \frac{1}{2} \tag{23}$$

Now, let v be the harmonic conjugate of u. Then the function

$$w = u + iv \tag{24}$$

is an analytic function of the complex variable

$$z = x + iy$$

and the functions u and v satisfy the Cauchy-Riemann equation. Upon taking u and v as new independent variables for equation (20) and introducing a new dependent variable Z defined by

$$Z \equiv \sqrt{\frac{\sinh H - \sin H}{\cosh H + \cos H}}\,\zeta \tag{25}$$

or by

$$Z = \zeta \qquad \text{for } h > \frac{1}{2} d \tag{26}$$

(if the approximations (23) are used) we find, after using the Cauchy-Riemann equations to simplify, that equation (20) becomes

$$Z_{uu} + Z_{vv} + 2\beta(u)Z_v - \left\{[\alpha(u)]' + [\alpha(u)]^2\right\}Z = \mathscr{F} \tag{27}$$

where

$$\mathscr{F} = \sqrt{\frac{\cosh H + \cos H}{\sinh H + \sin H}} \left[\sigma_x^{(1)} + \sigma_y^{(2)}\right] \left|\frac{dz}{dw}\right|^2 \tag{28}$$

When $h > \frac{1}{2} d$ the transformed equation can be approximated by

$$\left.\begin{aligned} &\zeta_{uu} + \zeta_{vv} + \frac{dH}{du} \zeta_v = \mathscr{F} \\ &\mathscr{F} = \left[\sigma_x^{(1)} + \sigma_y^{(2)}\right] \left|\frac{dz}{dw}\right|^2 \end{aligned}\right\} \quad \text{for } \frac{h}{d} > \frac{1}{2} \tag{29}$$

The details of the algebraic manipulations involved in obtaining equations (27) to (29) can be found in reference 3.

We are interested in solving equation (1) for a closed lake or sea that contains a single island. Thus, we shall seek solutions to equation (1) in the doubly connected region shown in figure 1 where the outer boundary (shore line) is $\mathscr{C}$ and where the inner (island) boundary is $\mathscr{S}$.

We shall suppose that the bottom topography of the basin can be approximately described by a function of the form (19) and that the depths along the shore lines $\mathscr{C}$ and $\mathscr{S}$ are both constants. Equation (19) now shows that the harmonic function u must also be constant along both $\mathscr{S}$ and $\mathscr{C}$. Without any loss of generality we can always redefine the functions H and u so that $u = 0$ on $\mathscr{C}$. We shall denote the constant value of u on $\mathscr{S}$ by u_s. Again, without loss of generality, it is always possible to arrange matters so that $u_s > 0$. Now, consider the analytic function w defined in terms of u by equation (24) and put

$$T = e^w \tag{30}$$

Then, T is an analytic function within the multiply connected region of figure 1 and since

$$|T| = e^u$$

it follows that $|T| = 1$ for z on $\mathscr{C}$ and $|T| = e^{u_s} = \text{constant}$ for z on $\mathscr{S}$. Hence the mapping

$$z \rightarrow T$$

transforms the multiply connected region of figure 1 into the interior of the concentric annular region in the T-plane shown in figure 2, with the outer boundary $\mathscr{C}$ mapping into the (inner) unit circle and the inner boundary $\mathscr{S}$ mapping into the outer circle with radius

$$R_o = e^{u_s} \tag{31}$$

On the other hand, as long as the boundaries of the regions shown in figure 1 are sufficiently smooth, the Reimann mapping theorem for doubly connected regions guarantees that there always exists an R_o for which such a mapping exists (ref. 4).

The mapping $w = \ln T$ transforms the cut annular region in the T-plane (see fig. 3) into the rectangular region in the w-plane shown in figure 4. Thus, u can always be chosen so that the analytic function w, defined in equation (24), maps the cut region occupied by the body of water shown in figure 5 into the rectangular regions in the w-plane shown in figure 4. The cut occurs along a line of constant v.

Now we have transformed equation (1) into equation (27) or, when $h > \frac{1}{2} d$, into equation (29) with u and v as the independent variables. Thus the problem of solving equation (1) for the lake configuration shown in figure 1 has been transformed into the problems of finding a solution to equation (27) or, alternatively, when $h > \frac{1}{2} d$ equation (29) in the rectangular region in the w-plane shown in figure 4. Although this simplifies the shape of the region in which the problem is to be solved, the most important simplification is due to the fact that all the coefficients in equations (27) and (29) are functions of only one of the independent variables. As will be shown subsequently, this will allow an analytical solution to the problem to be found.

Before this is done, however, it is first necessary to transform the boundary condition (18) in the physical plane into a boundary condition in the w-plane.

To this end, notice that since $u = 0$ on the boundary $\mathscr{C}$ and $u = u_s$ on $\mathscr{S}$ the unit normal vector $\hat{n}$ is given by

$$\hat{n} = \left(\frac{\nabla u}{|\nabla u|}\right)_{u=0} \qquad \text{on } \mathscr{C}$$

$$\hat{n} = \left(\frac{\nabla u}{|\nabla u|}\right)_{u=u_s} \qquad \text{on } \mathscr{S}$$

Hence, it follows from the Cauchy-Riemann conditions and the definition of the derivative of an analytic function that the components of n can be written as

$$
\left.\begin{aligned}
n_1 &= \frac{1}{\left|\frac{dw}{dz}\right|} \mathcal{R}e\left(\frac{dw}{dz}\right)^* = \frac{1}{\left|\frac{dw}{dz}\right|} \mathcal{R}e\left[\left(\frac{dw}{dz}\right)^* \frac{dw}{dz}\frac{dz}{dw}\right] = \left|\frac{dw}{dz}\right| \mathcal{R}e\,\frac{dz}{dw} \\
&\text{and} \\
n_2 &= \frac{1}{\left|\frac{dw}{dz}\right|} \mathcal{I}m\left(\frac{dw}{dz}\right)^* = \left|\frac{dw}{dz}\right| \mathcal{I}m\,\frac{dz}{dw}
\end{aligned}\right\} \tag{32}
$$

Thus, it follows from equations (12), (16), and (19) that boundary condition (18) can be written as

$$
\mathrm{Re}\left[\sigma + H(E + iF)\left(\frac{\partial\zeta}{\partial x} + i\,\frac{\partial\zeta}{\partial y}\right)\right]\left(\frac{dz}{dw}\right)^* = 0 \qquad \text{for } z \text{ on } \mathscr{C} \text{ and for } z \text{ on } \mathscr{S}
$$

After using the Cauchy-Riemann equations and the chain rule for partial derivatives, this becomes

$$
HF\,\frac{\partial\zeta}{\partial v} - HE\,\frac{\partial\zeta}{\partial u} = \mathrm{Re}\;\sigma\left(\frac{dz}{dw}\right)^* \quad \text{on } u = 0 \text{ and } u = u_s \text{ for } -\pi \le v \le \pi
$$

It now follows from equations (25), (6), (13), and (19) that Z must satisfy the following boundary conditions.

$$
\left.\begin{aligned}
p_o Z_u + q_o Z_v + s_o Z &= \gamma^{(o)}(v) \qquad \text{for } u = 0;\ -\pi \le v \le \pi \\
p_s Z_u + q_s Z_v + s_s Z &= \gamma^{(s)}(v) \qquad \text{for } u = u_s;\ -\pi \le v \le \pi
\end{aligned}\right\} \tag{33}
$$

where

$$\left.\begin{aligned}
p_o &= \frac{\sinh H(0) - \sin H(0)}{\cosh H(0) + \cos H(0)} \\
p_s &= \frac{\sinh H(u_s) - \sin H(u_s)}{\cosh H(u_s) + \cos H(u_s)} \\
q_o &= H(0) - \frac{\sinh H(0) + \sin H(0)}{\cosh H(0) + \cos H(0)} \\
q_s &= H(u_s) - \frac{\sinh H(u_s) + \sin H(u_s)}{\cosh H(u_s) + \cos H(u_s)} \\
s_o &= - \frac{\sin H(0) \sinh H(0)}{\left[\cos H(0) + \cosh H(0)\right]^2} \left(\frac{dH}{du}\right)_{u=0} \\
s_s &= - \frac{\sin H(u_s) \sinh H(u_s)}{\left[\cos H(u_s) + \cosh H(u_s)\right]^2} \left(\frac{dH}{du}\right)_{u=u_s}
\end{aligned}\right\} \qquad (34)$$

and

$$\left.\begin{aligned}
\gamma^{(o)}(v) &= \sqrt{\frac{\sinh H(0) - \sin H(0)}{\cosh H(0) + \cos H(0)}} \; \mathcal{R}e \left[\sigma \left(\frac{dz}{dw}\right)^*\right]_{u=0} \\
\gamma^{(s)}(v) &= \sqrt{\frac{\sinh H(u_s) - \sin H(u_s)}{\cosh H(u_s) + \cos H(u_s)}} \; \mathcal{R}e \left[\sigma \left(\frac{dz}{dw}\right)^*\right]_{u=u_s}
\end{aligned}\right\} \qquad (35)$$

When $h > \frac{1}{2} d$, equation (33) can be replaced by the approximate boundary conditions

$$\left.\begin{aligned}
p_o \zeta_u + q_o \zeta_v &= \gamma^{(o)}(v) \qquad \text{for } u = 0; \ -\pi \leq v \leq \pi \\
p_s \zeta_u + q_s \zeta_v &= \gamma^{(s)}(v) \qquad \text{for } u = u_s; \ -\pi \leq v \leq \pi
\end{aligned}\right\} \quad \text{for } \frac{h}{d} > \frac{1}{2} \qquad (36)$$

where now

$$\left.\begin{aligned} p_o &= p_s = 1 \\ q_o &= H(0) - 1 \\ q_s &= H(u_s) - 1 \end{aligned}\right\} \quad \text{for } \frac{h}{d} > \frac{1}{2} \tag{37}$$

and

$$\left.\begin{aligned} \gamma^{(o)}(v) &= \mathcal{R}e\left[\sigma\left(\frac{dz}{dw}\right)^{*}\right]_{u=0} \\ \gamma^{(s)}(v) &= \mathcal{R}e\left[\sigma\left(\frac{dz}{dw}\right)^{*}\right]_{u=u_s} \end{aligned}\right\} \quad \text{for } \frac{h}{d} > \frac{1}{2} \tag{38}$$

Since equation (27) is elliptic, it is still necessary to specify boundary conditions along the sides $v = \pm\pi$ of the rectangular region shown in figure 4. These conditions follow from the fact that ζ and its normal derivative must be continuous across the cut in the physical plane (see fig. 5). Since the opposite sides of this cut map into the lines $V = +\pi$ and $v = -\pi$, we must require that

$$\left.\begin{aligned} Z\left(u, \frac{\pi}{2}\right) &= Z\left(u, -\frac{\pi}{2}\right) \\ \text{and} \qquad & \\ \left(\frac{\partial Z}{\partial v}\right)_{v=\pi/2} &= \left(\frac{\partial Z}{\partial v}\right)_{v=-\pi/2} \end{aligned}\right\} \quad 0 \leq u \leq u_s \tag{39}$$

Or in view of equation (26) these can be replaced by the condition

$$\left.\begin{aligned} \zeta\left(u, \frac{\pi}{2}\right) &= \zeta\left(u, -\frac{\pi}{2}\right) \\ \left(\frac{\partial \zeta}{\partial v}\right)_{v=\pi/2} &= \left(\frac{\partial \zeta}{\partial v}\right)_{v=-\pi/2} \end{aligned}\right\} \quad 0 \leq u \leq u_s \qquad \text{for } \frac{h}{d} > \frac{1}{2} \tag{40}$$

when the approximate equation (29) is to be used.

We have now shown that the surface displacement for a sea or lake of arbitrary shape can be found by solving the differential equation (27) in the interior of the rectangular region shown in figure 4 subject to the boundary conditions (33) and the periodicity conditions (39). Or, if $h/d > 1/2$, the surface displacement is approximately obtained by solving equation (29) in the interior of the rectangular region in figure 4 subject to the boundary conditions (36) and the periodicity conditions (40).

Reduction to Ordinary Differential Equations and Summary

In order to solve the boundary value problem, we put

$$\Omega_n(u) \equiv \frac{1}{2\pi} \int_{-\pi}^{\pi} Z(u,v)e^{-inv}\, dv \qquad n = 0, \pm 1, \pm 2, \ldots \tag{41}$$

Then it follows from the theory of Fourier series that this transform can be inverted to obtain

$$Z(u,v) = \sum_{n=-\infty}^{\infty} \Omega_n(u)e^{inv} \tag{42}$$

On integrating by parts and using the periodicity conditions (39), we find that

$$\left.\begin{aligned} \frac{1}{2\pi} \int_{-\pi}^{\pi} Z_v(u,v)e^{-inv}\, dv &= in\Omega_n(u) \\ \frac{1}{2\pi} \int_{-\pi}^{\pi} Z_{vv}(u,v)e^{-inv}\, dv &= -n^2\Omega_n(u) \end{aligned}\right\} \tag{43}$$

We shall now show that each function Ω_n can be determined as the solution of a certain ordinary differential equation. To this end, multiply equations (27) and (33) by $e^{-inv}/2\pi$ and integrate both sides of the resulting expressions with respect to v between $-\pi$ and π. We find, on making the definitions

$$\left.\begin{aligned}\Gamma_n(u) &= \frac{1}{2\pi}\sqrt{\frac{\cosh H + \cos H}{\sinh H - \sin H}}\int_{-\pi}^{\pi} e^{-inv}\left[\sigma_x^{(1)} + \sigma_y^{(2)}\right]\left|\frac{dz}{dw}\right|^2 dv \\ \gamma_n(u) &= \frac{1}{2\pi}\sqrt{\frac{\sinh H - \sin H}{\cosh H + \cos H}}\int_{-\pi}^{\pi} e^{-inv}\,\mathcal{R}e\left[\sigma\left(\frac{dz}{dw}\right)^*\right]dv\end{aligned}\right\} \quad n = 0, \pm 1, \pm 2, \ldots \tag{44}$$

and using equations (43), that Ω_n must satisfy the ordinary differential equation

$$\Omega_n'' - (\alpha' + \alpha^2 + n^2 - 2in\beta)\Omega_n = \Gamma_n \qquad \begin{cases} n = 0, +1, +2, \ldots \\ 0 \le u \le u_s \end{cases} \tag{45}$$

subject to the boundary conditions

$$\left.\begin{aligned} p_o\Omega_n'(0) + (s_o + inq_o)\Omega_n(0) &= \gamma_n(0) \\ p_s\Omega_n'(u_s) + (s_s + inq_s)\Omega_n(u_s) &= \gamma_n(u_s)\end{aligned}\right\} \quad n = 0, \pm 1, \pm 2, \ldots \tag{46}$$

where p_o, q_o, s_o, p_s, q_s, and s_s are defined by equations (34) and equations (21) define α and β as

$$\left.\begin{aligned}\alpha &\equiv -\frac{\sin H \sinh H}{(\cos H + \cosh H)(\sin H - \sinh H)}\frac{dH}{du} \\ \beta &\equiv \frac{1}{2}\frac{\sinh H + \sin H}{\cosh H + \cos H}\frac{dH}{du}\end{aligned}\right\} \tag{21}$$

When $h/d > 1/2$, equations (44) to (21) (see eqs. (23) and (37) and ref. 3) can be replaced by the approximate equation.

$$\left.\begin{aligned}\Gamma_n(u) &= \frac{1}{2\pi}\int_{-\pi}^{\pi} e^{-inv}\left[\sigma_x^{(1)} + \sigma_y^{(2)}\right]\left|\frac{dz}{dw}\right|^2 dv \\ \gamma_n(u) &= \frac{1}{2\pi}\int_{-\pi}^{\pi} e^{-inv}\,\mathcal{R}e\left[\sigma\left(\frac{dz}{dw}\right)^*\right]dv\end{aligned}\right\} \quad n = 0, \pm 1, \pm 2, \ldots \qquad \text{for } \frac{h}{d} > \frac{1}{2} \tag{47}$$

$$\Omega_n'' - (n^2 - 2in\beta)\Omega_n = \Gamma_n \qquad \left\{ \begin{array}{l} n = 0, \pm 1, \pm 2, \ldots \\ 0 \leq u \leq u_s \end{array} \right\} \qquad \text{for } \frac{h}{d} > \frac{1}{2} \tag{48}$$

$$\left. \begin{array}{l} \Omega_n'(0) + in[H(0) - 1]\Omega_n(0) = \gamma_n(0) \\ \Omega_n'(u_s) + in[H(u_s) - 1]\Omega_n(u_s) = \gamma_n(u_s) \end{array} \right\} \quad n = 0, \pm 1, \pm 2, \ldots \qquad \text{for } \frac{h}{d} > \frac{1}{2} \tag{49}$$

$$\beta = \frac{1}{2}\frac{dH}{du} \qquad \text{for } \frac{h}{d} > \frac{1}{2} \tag{50}$$

Finally, equations (25) and (42) show that, once the systems (45) and (46) have been solved, the surface displacement can be found from the relation

$$\zeta = \sqrt{\frac{\cosh H + \cos H}{\sinh H - \sin H}} \sum_{n=-\infty}^{\infty} \Omega_n(u)e^{inv} \tag{51}$$

or when $h/d > 1/2$ approximated by

$$\zeta = \sum_{n=-\infty}^{\infty} \Omega_n(u)e^{inv} \qquad \text{for } \frac{h}{d} > \frac{1}{2} \tag{52}$$

Thus, an exact solution for the sea-level elevation (and, since all other physical quantities can be expressed in terms of this, an exact solution to the complete flow problem) can be obtained once the ordinary differential equation (45) with the boundary condition (46) has been solved. This solution is given parametrically in terms of the variables u and v. These parametric variables are determined in terms of the physical variables x and y by the mapping

$$z \rightarrow w$$

with $z = x + iy$ and $w = u + iv$, which maps the lake or sea conformally into the rectangular region in the w-plane shown in figure 4. The coefficients of the ordinary differential equation depend on the particular choice of the function $H(u)$. Thus it is impossible to proceed further in the general case.

The procedures involved in obtaining a complete solution are best illustrated by considering a particular case. In order to simplify the calculations it will be assumed that $h/d > 1/2$ and the approximate equations (47) to (50) will be used. A particular depth distribution function $H(u)$ will first be chosen. The ordinary differential equation will then be solved, and the surface displacement will be found as a function of u and v. A particular shape of the body of water and its island will then be chosen. Once this is done the relation between the physical variables x and y and the parametric variables u and v will be found. This will give the surface displacement as a function of x and y.

SOLUTION OF ORDINARY DIFFERENTIAL EQUATION FOR PARTICULAR BOTTOM TOPOGRAPHY

We shall consider the case where the function H of u is given by

$$H(u) = H_o + \frac{\delta}{u_s} u \qquad 0 \leq u \leq u_s \tag{53}$$

where H_o is the constant depth at the mainland shore and $H_o + \delta$ is the constant depth at the island shore. On inserting equation (53) into equations (48) to (50) we obtain

$$\Omega_n'' - \left(n^2 - \frac{in\delta}{u_s}\right)\Omega_n = \Gamma_n \qquad \begin{cases} n = 0, \pm 1, \pm 2, \; . \; . \; . \\ 0 \leq u \leq u_s \end{cases} \tag{54}$$

$$\left.\begin{aligned} \Omega_n'(0) + in(H_o - 1)\Omega_n(0) &= \gamma_n(0) \\ \Omega_n'(u_s) + in(H_o + \delta - 1)\Omega_n(u_s) &= \gamma_n(u_s) \end{aligned}\right\} \quad n = 0, \pm 1, \pm 2, \; . \; . \; . \tag{55}$$

Before obtaining the solution to this boundary value problem, we shall first show that

$$\int_0^{u_s} \Gamma_0(u)du = \gamma_0(u_s) - \gamma_0(0) \tag{56}$$

To this end notice that equations (47) imply

$$\left.\begin{aligned}
\Gamma_0 &= \frac{1}{2\pi}\int_{-\pi}^{\pi}\left[\sigma_x^{(1)} + \sigma_y^{(2)}\right]\left|\frac{dz}{dw}\right|^2 dv \\
\gamma_0(u_s) &= \frac{1}{2\pi}\int_{-\pi}^{\pi} \mathcal{R}e\left[\sigma\left(\frac{dz}{dw}\right)^*\right]_{u=u_s} dv \\
\gamma_0(0) &= \frac{1}{2\pi}\int_{-\pi}^{\pi} \mathcal{R}e\left[\sigma\left(\frac{dz}{dw}\right)^*\right]_{u=0} dv
\end{aligned}\right\} \tag{57}$$

Hence it follows from equation (24) and the Cauchy-Reimann equations that

$$\begin{aligned}
\int_0^{u_s}\Gamma_0(u)du &= \frac{1}{2\pi}\int_0^{u_s}\int_{-\pi}^{\pi}\left[\sigma_x^{(1)} + \sigma_y^{(2)}\right]\left|\frac{dz}{dw}\right|^2 du\, dv \\
&= \frac{1}{2\pi}\int_0^{u_s}\int_{-\pi}^{\pi}\left[\sigma_x^{(1)} + \sigma_y^{(2)}\right](x_u y_v - x_v y_u)du\, dv \\
&= \frac{1}{2\pi}\int_0^{u_s}\int_{-\pi}^{\pi}\left[\sigma_x^{(1)} + \sigma_y^{(2)}\right]\frac{\partial(x,y)}{\partial(u,v)} du\, dv
\end{aligned}$$

On recalling that the rectangular region in the w-plane over which this integration is performed transforms into the interior of the body of water in the z-plane, it follows from the theory of transformation of multiple integrals that

$$\int_0^{u_s}\Gamma_0(u)du = \frac{1}{2\pi}\iint\left[\sigma_x^{(1)} + \sigma_y^{(1)}\right]dx\, dy \tag{58}$$

where the integration is carried out over the entire surface occupied by the body of water. Let C denote the distance measured along the boundary $\mathscr{C}$ of this region; let S denote the distance measure along the boundary $\mathscr{S}$ of this region; and let the positive directions of C and S be counterclockwise and clockwise, respectively. Then applying the divergence theorem to equation (58) yields

$$\int_0^{u_s} \Gamma_0(u)du = \frac{1}{2\pi} \oint_{\mathscr{C}} \left[\sigma^{(1)}n_1 + \sigma^{(2)}n_2\right] dC + \frac{1}{2\pi} \oint_{\mathscr{S}} \left[\sigma^{(1)}n_1 + \sigma^{(2)}n_2\right] dS$$

Using equation (32) gives

$$\int_0^{u_s} \Gamma_0(u)du = \frac{1}{2\pi} \oint_{\mathscr{C}} \mathcal{Re}\left[\sigma\left(\frac{dz}{dw}\right)^*\right]\left|\frac{dw}{dz}\right| dC + \frac{1}{2\pi} \oint_{\mathscr{S}} \mathcal{Re}\left[\sigma\left(\frac{dz}{dw}\right)^*\right]\left|\frac{dw}{dz}\right| dS \qquad (59)$$

Now

$$|dS| = \sqrt{(dx)^2 + (dy)^2}$$

and

$$\left|\frac{dw}{dz}\right| = \sqrt{\left(\frac{\partial u}{\partial x}\right)^2 + \left(\frac{\partial v}{\partial x}\right)^2}$$

Hence

$$\left|\frac{dw}{dz}\right| |dS| = \sqrt{\left(\frac{\partial u}{\partial x} dx\right)^2 + \left(\frac{\partial v}{\partial x} dy\right)^2 + \left(\frac{\partial v}{\partial x} dx\right)^2 + \left(\frac{\partial u}{\partial x} dy\right)^2}$$

On using the Cauchy-Riemann equations and noting that $u_x u_y = -v_y v_x$ we find that

$$\left|\frac{dw}{dz}\right| |dS| = \sqrt{(u_x dx + u_y dy)^2 + (v_x dx + v_y dy)^2} = \sqrt{(du)^2 + (dv)^2}$$

But u is constant and equal to u_s on $\mathscr{S}$. Hence,

$$\left|\frac{dw}{dz}\right| |dS| = |dv|$$

or, taking into account the directions of transversal of the contours indicated in figures 4 and 5, we see that

$$\left|\frac{dw}{dz}\right| dS = dv$$

It also follows in the same way that

$$\left|\frac{dw}{dz}\right| dC = -dv$$

Equation (59) can therefore be written as

$$\int_0^{u_s} \Gamma_0(u)du = \frac{1}{2\pi} \int_{-\pi}^{\pi} \mathcal{R}e \left[\sigma\left(\frac{dz}{dw}\right)^*\right]_{u=u_s} dv - \frac{1}{2\pi} \int_{-\pi}^{\pi} \mathcal{R}e \left[\sigma\left(\frac{dz}{dw}\right)^*\right]_{u=0} dv$$

Finally, comparing this with equation (57) shows that equation (56) holds.

Having established this result, we can now proceed to solve the boundary value problem (eqs. (54) and (55)) for $n = 0$. In this case equations (54) and (55) become

$$\Omega_0'' = \Gamma_0 \tag{60}$$

and

$$\left.\begin{aligned} \Omega_0'(0) &= \gamma_0(0) \\ \Omega_0'(u_s) &= \gamma_0(u_s) \end{aligned}\right\} \tag{61}$$

Integrating equation (60) gives

$$\Omega_0' = \int_0^u \Gamma_0(t)dt + l_1$$

where l_1 is a constant of integration. On substituting this into the first boundary condition (61), we find that $l_1 = \gamma_0(0)$. Hence,

$$\Omega_0' = \int_0^u \Gamma_0(t)dt + \gamma_0(0) \tag{62}$$

Equations (56) now show that the second boundary condition (61) is automatically satisfied. Notice that it would be impossible to satisfy both boundary conditions (61) if equation (56) did not hold.

On the other hand, integrating equation (62) gives

$$\Omega_0 = l_0 + \int_0^u dt_1 \int_0^{t_1} \Gamma_0(t)dt + \gamma_0(0)u$$

where l_0 is a constant of integration. An integration by parts yields

$$\Omega_0(u) = l_0 + \gamma_0(0)u + \int_0^u (u - t)\Gamma_0(t)dt \tag{63}$$

Since both boundary conditions (61) are satisfied, the solution (63) is indeterminate to within an arbitrary constant l_0. But this is as it should be since the $n = 0$ term in equation (52) is independent of v and as can be seen from equations (29) and (36) the original boundary value problem for ζ involves only the partial derivatives of ζ and, hence, determines ζ only to within an arbitrary constant.

We now return to the boundary value problems (54) and (55) and suppose that $n \neq 0$. Put

$$\lambda_n = \sqrt{n^2 - \frac{in\delta}{u_s}} = \frac{n}{\sqrt{2}}\sqrt{\left[1 + \left(\frac{\delta}{nu_s}\right)^2\right]^{1/2} + 1} - \frac{i|n|}{\sqrt{2}}\sqrt{\left[1 + \left(\frac{\delta}{nu_s}\right)^2\right]^{1/2} - 1} \tag{64}$$

where for definiteness the branch cut has been chosen to lie along the imaginary n-axis between 0 and $i\delta/u_s$. Then, the general solution to equation (54) is

$$\Omega_n = l_1^{(n)}e^{\lambda_n u} + l_2^{(n)}e^{-\lambda_n u} + \frac{1}{\lambda_n}\int_0^u \sinh[\lambda_n(u - t)]\Gamma_n(t)dt \qquad n = \pm 1, \pm 2, \ . \ . \ . \tag{65}$$

where $l_1^{(n)}$ and $l_2^{(n)}$ are constants of integration. Substituting this expression into boundary conditions (55) shows that $l_1^{(n)}$ and $l_2^{(n)}$ satisfy the equations

$$l_1^{(n)}[\lambda_n + in(H_o - 1)] - l_2^{(n)}[\lambda_n - in(H_o - 1)] = \gamma_n(0)$$

$$l_1^{(n)}[\lambda_n + in(H_o + \delta - 1)]e^{\lambda_n u_s} - l_2^{(n)}[\lambda_n - in(H_o + \delta - 1)]e^{-\lambda_n u_s}$$

$$= \gamma_n(u_s) - \frac{1}{\lambda_n}\int_0^{u_s} [\lambda_n \cosh \lambda_n(u_s - t) + in(H_o + \delta - 1)\sinh \lambda_n(u_s - t)]\Gamma_n(t)dt$$

Solving these equations for $l_1^{(n)}$ and $l_2^{(n)}$ gives

$$\frac{l_1^{(n)}K_n}{\lambda_n - in(H_o - 1)} = J_n$$

$$\frac{l_2^{(n)}K_n}{\lambda_n + in(H_o - 1)} = J_n - \frac{\gamma_n(0)K_n}{\lambda_n^2 + n^2\left(H_o - 1\right)^2}$$

where we have put

$$K_n \equiv [\lambda_n - in(H_o - 1)][\lambda_n + in(H_o + \delta - 1)]e^{\lambda_n u_s}$$

$$- [\lambda_n + in(H_o - 1)][\lambda_n - in(H_o + \delta - 1)]e^{-\lambda_n u_s} \qquad n = \pm 1, \pm 2, \ldots \tag{66}$$

$$J_n \equiv \gamma_n(u_s) - \gamma_n(0)\left[\frac{\lambda_n - in(H_o + \delta - 1)}{\lambda_n - in(H_o - 1)}\right]e^{-\lambda_n u_s}$$

$$- \frac{1}{2\lambda_n}\int_0^{u_s} \omega_n(t - u_s; H_o + \delta)\Gamma_n(t)dt \qquad n = \pm 1, \pm 2, \ldots \tag{67}$$

and

$$\omega_n(u;\zeta) \equiv [\lambda_n - in(\zeta - 1)]e^{\lambda_n u} + [\lambda_n + in(\zeta - 1)]e^{-\lambda_n u} \qquad n = \pm 1, \pm 2, \ldots \tag{68}$$

Substituting these results into equation (65) now shows that

$$\Omega_n(u) = \frac{J_n}{K_n}\omega_n(u;H_o) - \frac{\gamma_n(0)e^{-\lambda_n u}}{\lambda_n - in(H_o - 1)} + \frac{1}{\lambda_n}\int_0^u \sinh[\lambda_n(u - t)]\Gamma_n(t)dt \qquad n = \pm 1, \pm 2, \ldots \tag{69}$$

Substituting equations (63) and (69) into equation (52) and noting that $[\Omega_n(u)]^* = \Omega_{-n}(u)$ gives

$$\zeta = l_0 + \gamma_0(0)u + \int_0^u (u - t)\Gamma_0(t)dt + 2\,\mathcal{Re}\sum_{n=1}^{\infty}\left\{\frac{J_n}{K_n}\omega_n(u;H_o) - \frac{\gamma_n(0)e^{-\lambda_n u}}{\lambda_n - in(H_o - 1)} + \frac{1}{\lambda_n}\int_0^u \sinh[\lambda_n(u - t)]\Gamma_n(t)dt\right\}e^{inv} \tag{70}$$

This gives the general solution to the problem in terms of the integrals $\Gamma_n(u)$ and $\gamma_n(u)$, which are defined in equations (47). It can be seen from equation (17) that, in order to evaluate these integrals, the complex wind stress τ^W and the function $z \to w$, which maps the interior of the body of water into the rectangular region in the w-plane (shown in fig. 4), must be specified. For lakes a good approximation is to take the wind stress as a constant. We shall therefore work out specific results only for this case and in the remainder of the report we will assume that τ^W is a complex constant. The function w can be found by the techniques of conformal mapping once the shape of the lake and island are specified.

Reduction of Integrals Γ_n and γ_n in the Case of Constant Wind Stress

When the wind stress τ^W is equal to a complex constant, it is possible to reduce the integrals (eq (44)) for Γ_n and γ_n to a form in which the only integrals that appear are contour integrals which depend only on the function w and not on the depth distribution H. In order to simplify the calculations we shall restrict ourselves to the approximate form (eq. (47)) with σ given by equations (17) and (19) for $h > \frac{1}{2}d$.

It is convenient to introduce the functions z and z^* as independent variables. Then, since w is analytic, w is a function of z only and not of z^*, and w^* is a function of z^* only and not of z. In addition, since

$$z = x + iy$$

and

$$z^* = x - iy$$

$$\left.\begin{aligned} \frac{\partial}{\partial z} &= \frac{1}{2}\left[\frac{\partial}{\partial x} - i\frac{\partial}{\partial y}\right] \\ \frac{\partial}{\partial z^*} &= \frac{1}{2}\left[\frac{\partial}{\partial x} + i\frac{\partial}{\partial y}\right] \end{aligned}\right\} \tag{71}$$

Then

$$\frac{\partial\sigma}{\partial z} = \frac{1}{2}\left[\frac{\partial\sigma^{(1)}}{\partial x} + \frac{\partial\sigma^{(2)}}{\partial y}\right] + \frac{i}{2}\left[\frac{\partial\sigma^{(2)}}{\partial x} - \frac{\partial\sigma^{(1)}}{\partial y}\right]$$

Hence,

$$\mathcal{Re}\,\frac{\partial\sigma}{\partial z} = \frac{1}{2}\left[\sigma_x^{(1)} + \sigma_y^{(2)}\right]$$

Since z is a function of w only and not of w^* this can be written as

$$\sigma_x^{(1)} + \sigma_y^{(2)} = 2\,\mathcal{Re}\left(\frac{\partial\sigma}{\partial w}\frac{dw}{dz}\right)$$

but, when τ^{W} is a constant, it follows from equations (17) and (19) that σ is a function of u only and independent of v. Hence,

$$\frac{\partial \sigma}{\partial w} = \frac{1}{2}\frac{d\sigma}{du}$$

and

$$\sigma_x^{(1)} + \sigma_y^{(2)} = \mathcal{R}e\left[\frac{d\sigma}{du}\frac{dw}{dz}\right] = \frac{1}{2}\left[\left(\frac{d\sigma}{du}\right)^*\left(\frac{dw}{dz}\right)^* + \frac{d\sigma}{du}\frac{dw}{dz}\right] \tag{72}$$

Also,

$$\mathcal{R}e\,\sigma\left(\frac{dz}{dw}\right)^* = \frac{1}{2}\left[\sigma\left(\frac{dz}{dw}\right)^* + \sigma^*\left(\frac{dz}{dw}\right)\right] \tag{73}$$

After inserting equations (72) and (73) into equation (47) and recalling that σ is independent of v and that

$$\left|\frac{dz}{dw}\right|^2 = \frac{dz}{dw}\left(\frac{dz}{dw}\right)^*$$

we get

$$\Gamma_n(u) = \frac{1}{2}\left[\left(\frac{d\sigma}{du}\right)^* \frac{1}{2\pi}\int_{-\pi}^{\pi} e^{-inv}\frac{dz}{dw}\,dv + \left(\frac{d\sigma}{du}\right)\frac{1}{2\pi}\int_{-\pi}^{\pi} e^{-inv}\left(\frac{dz}{dw}\right)^* dv\right]$$

$$\gamma_n(u) = \frac{1}{2}\left[\sigma^* \frac{1}{2\pi}\int_{-\pi}^{\pi} e^{-inv}\frac{dz}{dw}\,dv + \sigma\frac{1}{2\pi}\int_{-\pi}^{\pi} e^{-inv}\left(\frac{dz}{dw}\right)^* dv\right]$$

or, since $w = u + iv$,

$$\left.\begin{aligned}\Gamma_n(u) &= \frac{1}{2}\left[\left(\frac{d\sigma}{du}\right)^* e^{nu} I_n + \left(\frac{d\sigma}{du}\right) e^{-nu} I^*_{-n}\right] \\ \gamma_n(u) &= \frac{1}{2}\left[\sigma^* e^{nu} I_n + \sigma e^{-nu} I^*_{-n}\right]\end{aligned}\right\} \quad n = 0, \pm 1, \ldots \qquad \frac{h}{d} > \frac{1}{2} \tag{74}$$

where we have put

$$I_n \equiv \frac{1}{2\pi} \int_{-\pi}^{\pi} e^{-nw} \frac{dz}{dw} dv = \frac{1}{2\pi i} \int_{u-i\pi}^{u+i\pi} e^{-nw} \frac{dz}{dw} dw$$

It can be seen from figures 3 and 4 that by making the change of variable $w = \ln T$ we transform this integral into an integral about a closed contour, C_o, for example, in the T-plane. Thus

$$I_n = \frac{1}{2\pi i} \oint_{C_o} \frac{1}{T^n} \frac{dz}{dT} dT \tag{75}$$

where, since dz/dT has no singularities inside the annular region between the circles of radii R_o and 1, the contour C_o can be taken as any closed contour lying within this region and encircling the origin.

Now it is well known from the theory of functions that dz/dT must have a Laurent series expansion about the origin in the T-plane that converges in the annular region. It is easy to show that I_n is simply the coefficient of T^{n-1} in this series. In the general case an identical analysis beginning with equation (47) shows that

$$\left.\begin{aligned}\Gamma_n(u) &= \frac{1}{2}\sqrt{\frac{\cosh H + \cos H}{\sinh H - \sin H}}\left[\left(\frac{d\sigma}{du}\right)^* e^{nu} I_n + \left(\frac{d\sigma}{du}\right) e^{-nu} I^*_{-n}\right] \\ \gamma_n(u) &= \frac{1}{2}\sqrt{\frac{\sinh H - \sin H}{\cosh H + \cos H}}\left[\sigma^* e^{nu} I_n + \sigma e^{-nu} I^*_{-n}\right]\end{aligned}\right. \quad n = 0, \pm 1, \pm 2, \ldots$$

It follows from figures 1 and 2 and equation (75) that

$$I_0 = \frac{1}{2\pi i} \oint_{C_o} dz = 0$$

Hence,

$$\Gamma_0(u) = \gamma_0(u) = 0 \tag{76}$$

It follows from equations (17) and (19) that

$$\sigma = \frac{2\pi i \tau^W}{gd}\left\{2e^{-[(1+i)/2]H} - 1\right\} \qquad \text{for } \frac{h}{d} > \frac{1}{2} \tag{77}$$

Hence,

$$\frac{d\sigma}{du} = -\frac{2\pi i \tau^W}{gd}(1+i)e^{-[(1+i)/2]H}\frac{dH}{du} \qquad \text{for } \frac{h}{d} > \frac{1}{2} \tag{78}$$

Simplification of Solution for Surface Displacement in the Case of Constant Wind Stress

We shall now use the results obtained in the previous section to simplify solution (70) for the case where the wind stress τ^W is constant.

To this end notice that equations (63) and (76) show that

$$\Omega_0 = l_0 = \text{constant} \tag{79}$$

Now for $n \neq 0$ it follows from equation (64) that

$$\lambda_n^* = -\lambda_{-n} \tag{80}$$

and therefore equations (66) and (68) show that

$$\omega_n^* = -\omega_{-n} \tag{81}$$

$$K_n^* = -K_{-n} \tag{82}$$

Equations (67), (69), and (74) show that we can now write

$$J_n = \frac{1}{2} I^*_{-n} J^{(1)}_n + \frac{1}{2} I_n J^{(2)}_n$$

$$\Omega_n = \frac{1}{2} I^*_{-n} \Omega^{(1)}_n + \frac{1}{2} I_n \Omega^{(2)}_n \tag{83}$$

where

$$J^{(1)}_n \equiv \sigma(u_s) e^{-nu_s} - \sigma(0) \left[\frac{\lambda_n - in(H_o + \delta - 1)}{\lambda_n - in(H_o - 1)}\right] e^{-\lambda_n u_s} - \frac{1}{2\lambda_n} \int_0^{u_s} \omega_n(t - u_s; H_o + \delta) \frac{d\sigma}{dt} e^{-nt}\, dt \tag{84}$$

$$J^{(2)}_n = \sigma^*(u_s) e^{nu_s} - \sigma^*(0) \left[\frac{\lambda_n - in(H_o + \delta - 1)}{\lambda_n - in(H_o - 1)}\right] e^{-\lambda_n u_s} - \frac{1}{2\lambda_n} \int_0^{u_s} \omega_n(t - u_s; H_o + \delta) \left(\frac{d\sigma}{dt}\right)^* e^{nt}\, dt$$

$$\Omega^{(1)}_n = \frac{J^{(1)}_n}{K_n} \omega_n(u; H_o) - \frac{\sigma(0) e^{-\lambda_n u}}{\lambda_n - in(H_o - 1)} + \frac{1}{\lambda_n} \int_0^{u} \sinh[\lambda_n(u - t)] \frac{d\sigma}{dt} e^{-nt}\, dt \tag{85}$$

and

$$\Omega^{(2)}_n = \frac{J^{(2)}_n}{K_n} \omega_n(u; H_o) - \frac{\sigma^*(0) e^{-\lambda_n u}}{\lambda_n - in(H_o - 1)} + \frac{1}{\lambda_n} \int_0^{u} \sinh[\lambda_n(u - t)] \left(\frac{d\sigma}{dt}\right)^* e^{nt}\, dt$$

Equations (66), (80), and (82) now show that

$$\left[J_n^{(2)}\right]^* = J_{-n}^{(1)} - \frac{\sigma(0)K_{-n}}{[\lambda_{-n} - i(-n)(H_o - 1)][\lambda_{-n} + i(-n)(H_o - 1)]}$$

therefore, equations (66), (68), and (80) to (82) show that

$$\left[\Omega_n^{(2)}\right]^* = \Omega_{-n}^{(1)} \qquad \text{for } n = \pm 1, \pm 2, \ . \ . \ . \tag{86}$$

Recalling that (see remarks preceding eq. (70)) $\Omega_n^* = \Omega_{-n}$ and using equation (79) we find

$$\zeta = l_0 + 2\,\mathcal{R}e \sum_{n=1}^{\infty} \Omega_n(u) e^{inv}$$

Substituting equation (83) into this expression gives

$$\zeta = l_0 + \mathcal{R}e \sum_{n=1}^{\infty} I_{-n}\Omega_n^{(1)}(u)e^{inv} + \mathcal{R}e \sum_{n=1}^{\infty} I_n\Omega_n^{(2)}(u)e^{inv}$$

Since for any complex number M, $\mathcal{R}e\, M^* = \mathcal{R}e\, M$, this becomes

$$\zeta = l_0 + \mathcal{R}e \sum_{n=1}^{\infty} I_{-n}^*\Omega_n^{(1)}(u)e^{inv} + \mathcal{R}e \sum_{n=1}^{\infty} I_n^*\left[\Omega_n^{(2)}(u)\right]^* e^{-inv}$$

Finally, using equation (86) and the fact that $I_o = 0$, shows that

$$\zeta = l_0 + \mathcal{R}e \sum_{n=-\infty}^{\infty} I_{-n}^*\Omega_n^{(1)}(u)e^{inv} \tag{87}$$

After integrating by parts equation (84) becomes

$$J_n^{(1)} = \frac{\sigma(0)K_n}{2\lambda_n[\lambda_n - in(H_o - 1)]} + \frac{1}{2\lambda_n}\int_0^{u_s} \sigma \frac{d}{dt}\left[\omega_n(t - u_s; H_o + \delta)e^{-nt}\right]dt$$

Substituting this into equation (85) and performing another integration by parts yield

$$\Omega_n^{(1)} = \frac{\omega_n(u; H_o)}{2\lambda_n K_n} \int_0^{u_s} \sigma \frac{d}{dt}\left[\omega_n(t - u_s; H_o + \delta) e^{-nt}\right] dt$$

$$- \frac{1}{\lambda_n} \int_0^{u} \sigma \frac{d}{dt}\left[e^{-nt} \sinh \lambda_n(u - t)\right] dt \qquad (88)$$

Substituting equation (53) into equation (77) and using the result in equation (88), gives

$$\Omega_n^{(1)} = \frac{2\pi i \tau^w}{gd} \left\{ \frac{\omega_n(u; H_o)}{\lambda_n K_n} \int_0^{u_s} e^{-\left(\frac{1+i}{2}\right)\left(H_o + \frac{\delta}{u_s} t\right)} \frac{d}{dt}\left[e^{-nt}\, \omega_n(t - u_s; H_o + \delta)\right] dt \right.$$

$$- \frac{2}{\lambda_n} \int_0^{u} e^{-\left(\frac{1+i}{2}\right)\left(H_o + \frac{\delta}{u_s} t\right)} \frac{d}{dt}\left[e^{-nt} \sinh \lambda_n(u - t)\right] dt$$

$$\left. - \frac{1}{K_n}\left[e^{-nu_s}\, \omega_n(u; H_o) - \omega_n(u - u_s; H_o + \delta)\right] \right\}$$

Since

$$\int_0^{u_s} e^{\left(\frac{1+i}{2}\right)\frac{\delta}{u_s}t} \frac{d}{dt}\left[e^{-nt}\,\omega_n(t - u_s; H_o + \delta)\right]dt$$

$$= \frac{(\lambda_n - n)[\lambda_n - in(H_o + \delta - 1)]}{n - \lambda_n + \left(\frac{1+i}{2}\right)\frac{\delta}{u_s}}\left\{e^{-\lambda_n u_s} - e^{-\left[nu_s + \left(\frac{1+i}{2}\right)\delta\right]}\right\}$$

$$- \frac{(\lambda_n + n)[\lambda_n + in(H_o + \delta - 1)]}{n + \lambda_n + \left(\frac{1+i}{2}\right)\frac{\delta}{u_s}}\left\{e^{\lambda_n u_s} - e^{-\left[nu_s + \left(\frac{1+i}{2}\right)\delta\right]}\right\}$$

$$= \frac{n\delta\lambda_n(1 + i)[2 + i(H_o + \delta)]}{u_s\left\{\left[n + \left(\frac{1+i}{2}\right)\frac{\delta}{u_s}\right]^2 - \lambda_n^2\right\}} e^{-\left[nu_s + \left(\frac{1+i}{2}\right)\delta\right]}$$

$$+ \frac{(\lambda_n + n)[\lambda_n + in(H_o + \delta - 1)]}{n - \lambda_n + \left(\frac{1+i}{2}\right)\frac{\delta}{u_s}} e^{-\lambda_n u_s}$$

$$- \frac{(\lambda_n + n)[\lambda_n + in(H_o + \delta - 1)]}{n + \lambda_n + \left(\frac{1+i}{2}\right)\frac{\delta}{u_s}} e^{\lambda_n u_s}$$

and

$$\int_0^u e^{-\left(\frac{1+i}{2}\right)\frac{\delta}{u_s}t} \frac{d}{dt}[e^{-nt} \sinh \lambda_n(u - t)]dt$$

$$= \frac{\delta\lambda_n(1 + i)}{2u_s\left\{\left[n + \left(\frac{1 + i}{2}\right)\frac{\delta}{u_s}\right]^2 - \lambda_n^2\right\}} e^{-\left[n+\left(\frac{1+i}{2}\right)\frac{\delta}{u_s}\right]u}$$

$$+ \frac{n - \lambda_n}{2\left[n - \lambda_n + \left(\frac{1 + i}{2}\right)\frac{\delta}{u_s}\right]} e^{-\lambda_n u} - \frac{(n + \lambda_n)}{2\left[n + \lambda_n + \left(\frac{1 + i}{2}\right)\frac{\delta}{u_s}\right]} e^{\lambda_n u}$$

It follows that

$$\Omega_n^{(1)} = \frac{2\pi i \tau^w}{gd} \Omega_n^{(0)} \tag{89}$$

where we have put

$$\Omega_n^{(0)} = \frac{1}{K_n}\left[\omega_n(u; H_o)M_n(H_o + \delta)e^{-nu_s} - \omega_n(u - u_s; H_o + \delta)M_n(H_o)\right]$$

$$- \frac{\delta(1+i)e^{-\left[nu+\left(\frac{1+i}{2}\right)H\right]}}{u_s\left\{\left[n + \left(\frac{1 + i}{2}\right)\frac{\delta}{u_s}\right]^2 - \lambda_n^2\right\}}$$

and

$$M_n(\zeta) \equiv \frac{n\delta(1+i)[2+i\zeta]}{u_s\left\{\left[n+\left(\frac{1+i}{2}\right)\frac{\delta}{u_s}\right]^2 - \lambda_n^2\right\}} e^{-\left(\frac{1+i}{2}\right)\zeta} - 1$$

Since

$$\left[n+\left(\frac{1+i}{2}\right)\frac{\delta}{u_s}\right]^2 - \lambda_n^2 = \frac{(1+i)\delta}{2u_s}\left[2n+(1+i)\left(n+\frac{1}{2}\frac{\delta}{u_s}\right)\right]$$

substituting equation (89) into equation (87) gives

$$\zeta = l_0 + \mathcal{Re}\,\frac{2\pi i\tau^W}{gd}\sum_{n=-\infty}^{\infty} I^*_{-n}\Omega_n^{(0)}(u)e^{inv} \tag{90}$$

where

$$\Omega_n^{(0)} = \frac{1}{K_n}\left[\omega_n(u;H_o)M_n(H_o+\delta)e^{-nu_s} - \omega_n(u-u_s;H_o+\delta)M_n(H_o)\right] - \frac{2e^{-\left[nu+\left(\frac{1+i}{2}\right)H(u)\right]}}{2n+(1+i)\left(n+\frac{1}{2}\frac{\delta}{u_s}\right)} \tag{91}$$

$$\omega_n(u;\zeta) \equiv [\lambda_n - in(\zeta-1)]e^{\lambda_n u} + [\lambda_n + in(\zeta-1)]e^{-\lambda_n u} \tag{68}$$

$$K_n \equiv [\lambda_n - in(H_o-1)][\lambda_n + in(H_o+\delta-1)]e^{\lambda_n u_s} - [\lambda_n + in(H_o-1)][\lambda_n - in(H_o+\delta-1)]e^{-\lambda_n u_s} \tag{66}$$

$$M_n(\zeta) = \frac{2n(2 + i\zeta)}{2n + (1 + i)\left(n + \frac{1}{2}\frac{\delta}{u_s}\right)} e^{-\left(\frac{1+i}{2}\right)\zeta} - 1 \tag{92}$$

$$I_n = \frac{1}{2\pi i} \oint_{C_o} \frac{1}{T^n} \frac{dz}{dT} dT \tag{75}$$

This gives the solution to the problem for the case of a constant wind stress. Numerical results can be obtained once the constants I_n are specified. These constants depend only on the shape of the lake and island, and it is only through these constants that the specific lake and island geometry enter the problem. They can be determined once the mapping $z \rightarrow T$ of the region occupied by the body of water into the annular region of figure 2 is known. The constants I_n are then determined either by evaluating the contour integral (75) or by finding the coefficients of the Laurent series expansion of the mapping about the origin in the T-plane.

Since $w = \ln T$, a knowledge of the mapping $z \rightarrow T$ is equivalent to a knowledge of the mapping $z \rightarrow w$, which transforms the cut region occupied by the body of water shown in figure 5 into the rectangular region in the w-plane shown in figure 4. This mapping can be used to express the variables u and v in the w plane as functions of x and y. Since equation (90) gives the surface displacement as a function of u and v, a knowledge of the mapping $z \rightarrow w$ allows us to express the surface displacement parametrically as a function of position in the physical plane. In order to illustrate these ideas a complete numerical solution will be worked out for a specific geometry.

Solution of Complete Boundary Value Problem for a Circular Lake Containing an Eccentricity Located Circular Island With an Imposed Constant Wind Stress

In order to find the mapping $z \rightarrow w$ the specific shape of the body of water and its island must be specified. We shall, therefore, suppose that the body of water is a circle with radius r and that the island is also a circle whose radius is r_S. However, the center of the island and the center of the lake do not necessarily coincide. The plan view of the lake and island are shown in figure 6. As discussed, the slit is included in the figure, and with no loss in generality we have chosen the x-axis to lie along the line of center of the island and the lake. In order to find the analytic function w with the appropriate properties it is necessary to map the cut eccentric annular region shown in figure 6 into the rectangular region in figure 4 in the manner indicated in the figures. This is best accomplished by first finding the mapping $z \rightarrow T$, which transforms the eccentric annular region in the z-plane (fig. 6) into the concentric annular region in the T-plane as shown in figure 3. But this mapping is given in reference 4 (p. 287) as

$$T = \frac{z - ar}{az - r} \tag{93}$$

where a is related to the coordinates x_a and x_b of the island shown in figure 6 by

$$a = \frac{1 + \left(\frac{x_a}{r}\right)\left(\frac{x_b}{r}\right) + \sqrt{\left[1 - \left(\frac{x_a}{r}\right)^2\right]\left[1 - \left(\frac{x_b}{r}\right)^2\right]}}{\left(\frac{x_a}{r}\right) + \left(\frac{x_b}{r}\right)} \tag{94}$$

with $a > 1$ and where the radius of the larger circle in the T-plane (shown in figs. 2 and 3) must be equal to

$$R_o = \frac{1 - \left(\frac{x_a}{r}\right)\left(\frac{x_b}{r}\right) + \sqrt{\left[1 - \left(\frac{x_a}{r}\right)^2\right]\left[1 - \left(\frac{x_b}{r}\right)^2\right]}}{\left(\frac{x_a}{r}\right) - \left(\frac{x_b}{r}\right)} \tag{95}$$

Since $w = \ln T$ it follows from equation (93) that

$$w = u + iv = \ln\left(\frac{z - ar}{az - r}\right) \qquad z = x + iy \tag{96}$$

Hence, for each value of the point x, y in the region occupied by the body of water in figure 6 we can compute a point (u, v) in the rectangular region of figure 4. For this value of u and v, we can find a value of the surface displacement ζ from equation (90). This determines ζ as a function of position in the physical (z-plane) plane.

It only remains to determine the constants I_n. To this end we solve equation (93) for z to obtain

$$z = r\,\frac{a - T}{1 - aT}$$

Differentiating with respect to T gives

$$\frac{dz}{dT} = r \frac{a^2 - 1}{(1 - aT)^2}$$

On inserting this into equation (75) we obtain

$$I_n = r(a^2 - 1) \frac{1}{2\pi i} \oint_{C_o} \frac{1}{T^n(1 - aT)^2} dT \qquad n = \pm 1, \pm 2, \ldots \tag{97}$$

where C_o is any contour encircling the origin and lying between the unit circle and the circle of radius R_o in the T-plane (fig. 2). This integral can easily be evaluated by the method of residues. Since $a > 1$ the pole of order two of the integrand at the point $T = 1/a$ lies within the unit circle and therefore within the contour C_o. In addition for $n > 0$, I_n has a pole of order n within C_o at $T = 0$, but this pole will not occur when $n \leq 0$.

In order to evaluate the residue at $T = 0$, we expand $(1 - aT)^{-2}$ in a Taylor series about $T = 0$ to obtain

$$\frac{1}{(1 - aT)^2} = \sum_{m=0}^{\infty} (m + 1)(aT)^m$$

Hence the integrand has the Laurent expansion about $T = 0$:

$$\frac{1}{T^n(1 - aT)^2} = \sum_{m=0}^{\infty} (m + 1)a^m T^{m-n}$$

The coefficient of T^{-1} is na^{n-1}; hence, at $T = 0$ the residue of the integral in equation (97), $\mathcal{Res}(T = 0)$ is

$$\mathcal{Res}(T = 0) = \begin{cases} na^{n-1} & \text{for } n = 1, 2, \ldots \\ 0 & \text{for } n = 0, -1, -2, \ldots \end{cases}$$

The residue $\mathcal{Res}\left(T = \frac{1}{a}\right)$ at $T = \frac{1}{a}$ is

$$\mathcal{Res}\left(T = \frac{1}{a}\right) = \left(\frac{d}{dT}\frac{1}{a^2 T^n}\right)_{T=1/a} = -na^{n-1} \qquad \text{for } n = 0, \pm1, \pm2, \ldots$$

Hence, on taking the sum of the residues and using the residue theorem, we find that

$$I_n = \begin{cases} -r(a^2 - 1)na^{n-1} & \text{for } n = -1, -2, \ldots \\ 0 & \text{for } n = 0, 1, 2, \ldots \end{cases}$$

$$I^*_{-n} = \begin{cases} \dfrac{r(a^2 - 1)n}{a^{n+1}} & \text{for } n = 1, 2, \ldots \\ 0 & \text{for } n = 0, -1, -2, \ldots \end{cases} \tag{98}$$

Equation (98) gives the values of the constants that are needed for equation (90) to compute the surface displacement.

Computation of Flow Field from Surface Displacement

Having solved for the surface displacement, the other quantities of physical interest can be calculated. These quantities are the complex horizontal velocity $U + iV$ which is given in terms of the surface displacement by equation (10) and the depth averaged velocity Q, which is given in terms of this surface displacement by equation (14).

Since the surface displacement is computed first as a function of u and v, it is convenient to express the other quantities as functions of u and v and then use equation (96) to relate them to x and y.

In order to accomplish this, we use equation (71) to write

$$\zeta_x + i\zeta_y = 2\frac{\partial\zeta}{\partial z^*}$$

but, since w is analytic, w^* is a function of z^* only. Hence,

$$\zeta_x + i\zeta_y = 2\,\frac{\partial \zeta}{\partial w^*}\left(\frac{dw}{dz}\right)^* = (\zeta_u + i\zeta_v)\left(\frac{dw}{dz}\right)^* \tag{99}$$

Inserting this together with equation (19) into equation (10) now yields

$$(U + iV)\,\frac{f_c}{g} = \left[\frac{(1 - i)\pi\tau^w}{gd}\right]\frac{\sinh\left\{\left(\frac{1 + i}{2}\right)\left[H(u) + \frac{2\pi\xi}{d}\right]\right\}}{\cosh\left[\left(\frac{1 + i}{2}\right)H(u)\right]}$$

$$- i\left\{\frac{\cosh\left[\left(\frac{1 + i}{2}\right)\frac{2\pi\xi}{d}\right]}{\cosh\left[\left(\frac{1 + i}{2}\right)H(u)\right]} - 1\right\}\left(\frac{\partial \zeta}{\partial u} + i\,\frac{\partial \zeta}{\partial v}\right)\left(\frac{dw}{dz}\right)^* \tag{100}$$

Upon noting that $T = e^w$, we find that

$$\frac{dz}{dw} = \frac{dz}{dT}\,\frac{dT}{dw} = e^w\,\frac{dz}{dT}$$

It now follows from equation (97) that the term $(dw/dz)^*$ in equation (100) can be expressed as a function of u and v by

$$\left(\frac{dw}{dz}\right)^* = \frac{\left(1 - ae^{w^*}\right)^2}{r\left(a^2 - 1\right)e^{w^*}} \qquad w^* = u - iv \tag{101}$$

Thus, equations (90), (100), and (101) give $u + iv$ as a function of u and v and ξ.

In a similar way we can substitute equations (19) and (99) into equation (14) to express Q as a function of u and v:

$$\frac{2\pi Q f_c}{gd} = \sigma - \left\{1 + i[1 - H(u)]\right\}(\zeta_u + i\zeta_v)\left(\frac{dw}{dz}\right)^* \tag{102}$$

However, instead of working with the volume flow itself, it is more convenient for plotting purposes to find the stream function. In reference 1 it is shown that Q_1 and Q_2 satisfy the continuity equation

$$\frac{\partial Q_1}{\partial x} + \frac{\partial Q_2}{\partial y} = 0$$

Hence, there exists a stream function ψ such that

$$\left.\begin{aligned} Q_1 &= \frac{\partial \psi}{\partial y} \\ Q_2 &= -\frac{\partial \psi}{\partial x} \end{aligned}\right\} \tag{103}$$

Hence

$$Q = \frac{\partial \psi}{\partial y} - i\frac{\partial \psi}{\partial x} = \frac{1}{i}(\psi_x + i\psi_y) = \frac{2}{i}\frac{\partial \psi}{\partial z^*} = \frac{2}{i}\frac{\partial \psi}{\partial w^*}\left(\frac{dw}{dz}\right)^* = \frac{1}{i}\left(\frac{\partial \psi}{\partial u} + i\frac{\partial \psi}{\partial v}\right)\left(\frac{dw}{dz}\right)^*$$

Inserting this into equation (102) dividing through by $1/i\ (dw/dz)^*$ and taking the real part gives

$$\frac{2\pi f_c}{gd}\frac{\partial \psi}{\partial u} = \left[\mathcal{R}e\ i\sigma\left(\frac{dz}{dw}\right)^*\right] + [1 - h(u)]\zeta_u + \zeta_v \tag{104}$$

Since the normal volume flow vanishes at the boundaries the boundaries themselves must be streamlines. Hence ψ must be constant along each boundary. Since ψ is only determined by equation (103) to within an arbitrary constant, we can set it equal to zero along the mainland coast $\widehat{12}$ in figure 6. Since this line maps into the line $u = 0$ in the w-plane (fig. 4) it follows that

$$\psi(0, v) = 0 \qquad -\pi \leq v \leq \pi$$

Hence, equation (104) can be integrated along a line of constant v to obtain

$$\frac{2\pi f_c}{gd}\psi(u, v) = \mathcal{R}e\ i\int_0^u \sigma\left(\frac{dz}{dw}\right)^* du + \int_0^u [1 - h(u)]\frac{\partial \zeta}{\partial u}du + \frac{\partial}{\partial v}\int_0^u \zeta\, du \tag{105}$$

which together with equations (17), (90), and (101) allow us to compute ψ as a function of u and v.

DISCUSSION OF RESULTS

A method for obtaining solutions to a certain class of partial differential equations in a doubly connected domain is given. This class of equation includes the equation for the wind-driven circulation in shallow seas and lakes for a large class of bottom topographies. The technique is used to reduce the problem of finding solutions to the shallow sea equation for a closed body of water with an island to the problem of solving an ordinary differential equation. An approximate form of this ordinary differential equation, which is valid when the depth of the body of water is greater than one half of the Ekman depth, is solved for a particular bottom topography and a constant wind shear stress.

The results presented herein are for a circular lake containing a concentrically or eccentrically located circular island with a logarithmic bottom topography. Two classes of bottom topography are included: One where the lake is deepest at the mainland shore and the other where the lake is deepest at the island shore. The assumption that the water depth is greater than one half the Ekman thickness is quite realistic. For instance in Lake Erie, which is the most shallow of the Great Lakes, only some 15 percent of the total bottom in the central and eastern basin is less than 1/2 the Ekman thickness for a 10 meter per second (22 mph) wind.

The surface displacement of the body of water is given in terms of the intermediate variables u and v by equation (90) with the aid of equations (91), (68), (66), (92), and (98). The horizontal velocity as a function of u and v and depth ξ is given by equation (100) and the stream function ψ as a function of just u and v is given by equation (105). Since the physical coordinates x and y of the horizontal plane of the body of water are related to the intermediate variables u and v parametrically by equation (96), the surface displacement, the horizontal velocity, and the stream function are known as functions of x and y. The solution for ζ, U, V, and ψ depend on the wind shear stress τ^W, the friction depth d, the bottom depth $h(x,y)$, the basin radius, the island diameter $(x_a - x_b)/r$, and the eccentricity of the island defined as $(x_a + x_b)/2r$. The magnitude of the wind stress $|\tau^W|$ enters only as a normalizing parameter in the solutions. Table I contains a list of the various solutions for which results are given herein.

The bottom topography with an island diameter of 0.5, island eccentricity of 0, $h/d = 1.0$ at the mainland shore, and $h/d = 0.5$ at the island is shown in figure 7(a). This topography includes the main effects due to an island. In an actual basin without an island, the depth is smallest at the mainland shore and largest at some central interior point. Islands create local areas in the interior of the basin where the depth becomes shallow. The topography shown in figure 7(a) will therefore give the local effect due to the island.

TABLE I. - CIRCULAR BASIN SOLUTIONS

Figure number	Depth ratio, h/d		Island eccentricity, $(x_a + x_b)/(2r)$	Island diameter, $(x_a - x_b)/r$	$\tau^w/\lvert\tau^w\rvert$
	At mainland shore	At island shore			
7	1.0	0.5	0	0.50	i
8	1.0	.5	.5	.50	i
9	1.0	.5	.5	.50	1.0
10	1.0	.5	0	.25	i
11	3.0	.5	0	.50	i
12	.5	1.0	0	.50	i
13	.5	3.0	0	.50	i
14	.5	3.0	0	.25	i
15	.5	1.0	.5	.50	1.0
16	.5	1.0	↓	↓	i
17	.5	3.0	↓	↓	1.0
18	.5	3.0	↓	↓	i
19	3.0	.5	↓	↓	1.0
20	3.0	.5	↓	↓	i

The surface displacement caused by a wind in the positive y-direction for the bottom topography depicted in figure 7(a) is shown in figure 7(b). Gedney (ref. 2) has shown that the solution for a constant depth basin is the same whether or not an island is present. As is well known, the surface displacement solution for a constant depth basin is a plane inclined to the horizontal. The deviation of the surface displacement shown in figure 7(b) is then the effect of the variations in bottom depth. Although the deviations of the surface displacement from an inclined plane are small, they will have major effects in the local velocities.

The horizontal volume flow stream function is shown in figure 7(c) for the case under discussion. The stream function plot consists of two gyres; the gyre to the right of the wind is rotating clockwise and the one to the left of the wind is rotating counterclockwise. The two gyres are separated by a dividing streamline, which in this case has a value of zero. The value of ψ on both the island and mainland shores is zero, and the zero streamline in the interior has been twisted relative to the wind in a clockwise direction.

As shown in the ψ plots in reference 2, the dividing streamline for a dish shaped basin whose depth increases monotonically from the shore to some interior point always runs through the maximum depth point. If the depth decreases monotonically from the shore to an interior point, the dividing streamline would run through the minimum depth point. In the case of the island shown in figure 7(c), the zero streamline runs through the minimum depth point interior to the mainland shore which happens to be the island boundary. If the island was not placed at the minimum depth point, the ψ value on the island boundary would assume some other value; that is, the path of the streamline dividing the two gyres is determined primarily by the extremes in the bottom topography.

The horizontal velocities at $\xi/d = 0$, -0.125, -0.250, -0.375, and -0.500 are shown in figures 7(d) to (h). The magnitude of each velocity vector plotted can be determined from the scale included on the plot. The origin of the velocity vector is the position at which velocity is actually occurring. The velocities at the surface are skewed to the right of the wind mainly because of the Coriolis force. Local perturbations in the surface velocities due to the volume flow gyres are evident. The acceleration of the velocities around the island and the deceleration near $x = -1$ and $+1$ can be directly attributed to the volume flow gyres shown in figure 7(c). At $\xi/d = -0.125$ mass is still being transported in the direction of the wind but an increasing amount is being transported to the right of the wind. The flow acceleration around the island is still evident. At $\xi/d = -0.25$ the flow pattern is very similar to that of the integrated volume flow shown in figure 7(c). Return flow opposite to the wind direction is now occurring. The flow near the island is predominately tangent to it. At $\xi/d = -0.375$ and -0.50 there is much return flow opposite in direction to the top surface layer flow. The flow below $\xi/d = -0.50$ is very similar in direction but decreases in magnitude from that shown at $\xi/d = -0.50$. This general flow pattern where mass in the top surface layer is transported in the direction of and to the right of the wind and returned in the opposite direction in the bottom layer is the dominant pattern in shallow lakes. The variations in this general pattern are due to the particular bottom topography. For this particular case where the bottom slopes upwards at the island an acceleration of flow occurs around the island.

The effect of offsetting the island relative to the center of the basin is shown in figure 8. The bottom topography, as shown in figure 8(a), has the same values at the mainland and island as the previous case but the center of the island is at $x/r = 0.5$. The wind direction and island diameter are the same for the two cases shown in figures 7 and 8. The effect of the eccentricity on the stream function is clearly shown in figure 8(c). The zero streamline still runs around the island shore since this is still the shallowest point in the lake. The gyres though no longer symmetric still have the same overall behavior as the concentric island case. Comparing the velocity plots shown in figures 8(d) to (h) with the ones in figure 7 shows that the flow patterns are essentially the same type for both cases. Making the island eccentric has the main effect of locally contracting and expanding the patterns for the concentric island case.

Figure 9 gives the results for an island diameter of 0.5, an eccentricity of 0.5, $h/d = 1.0$ at the mainland shore, $h/d = 0.5$ at the island shore, and with the wind along the x-axis. In the concentric island case the bottom topography is independent of the angle about the origin of the x,y axes. As a result, the solutions for any two wind directions are the same except rotated by the difference in wind angles. Therefore, it is possible to compare the results shown in figure 7 with those in figure 9 to determine the effect of an eccentric island when the wind is along the x-axis. As in the case where the wind is in the direction of the y-axis, the effect of locating the island eccentrically when the wind is along the x-axis is to cause a local contraction and expansion of the patterns which occur in the concentric island case.

The effect of change in island size can be seen by comparing figure 7 and figure 10. The results shown in these figures are for the same parameters except the island diameter is 0.5 in the case of figure 7 and 0.25 in the case of figure 10. The bottom topographies for these two cases are very nearly the same when plotted against distance from the island shore. As a result, for points equidistant from the island shore the velocities in the two cases are very nearly the same in magnitude and direction. This just illustrates again the importance of bottom topography.

The combined effect of making the basin deeper and the bottom slopes greater is demonstrated in figure 11. Here $h/d = 3.0$ at the mainland shore, and $h/d = 0.50$ at the island as shown in figure 11(a). Figure 11(b) shows first that the average surface displacement slope is much smaller than for the case shown in figure 7(b). This, of course, is because the basin shown in figure 11 has a greater average depth than the basin shown in figure 7. However, the surface displacement perturbation due to the change in bottom depth are much greater in figure 11(b) than figure 7(b). This effect is due to the larger bottom slopes in the case shown in figure 11.

The effects of larger depths and bottom slopes on the stream function can be determined by comparing figures 11(c) and 7(c). First, the zero streamline is twisted clockwise relative to the wind by a much greater angle in the case shown in figure 11(c). Second, the value of the stream function gradients are much greater in figure 11(c), creating larger volume flows.

The stream function effects just mentioned produce the major differences between the flow velocities in figures 11(d) to (h) from those in figures 7(d) to (h). Because the zero streamline in figure 11 is more perpendicular than parallel to the wind, the flow near the surface and bottom are more alined to the horizontal axis than in figure 7. Also in figure 11 there is a greater acceleration of velocities around the island.

When the sign of the bottom slope ($\partial h/\partial x$, $\partial h/\partial y$) is reversed, we can expect a significant change. In figure 12, the results are given for $h/d = 0.5$ at the mainland shore, $h/d = 1.0$ at the island, eccentricity = 0 and island diameter = 0.5. The average surface displacement slope in figure 12(b) is greater than in figure 7(b) because the average depth in the case shown in figure 12 is less than in the case shown in figure 7. There are differences in the deviations from a constant slope surface displacement between the two cases although they are not easily discernible.

The effect of changing the sign of the bottom slope can be more readily seen by comparing the stream function plots in figures 12(c) and 7(c). When for $x < 0$ $\partial h/\partial x$ is positive as in the case of figure 12 the zero streamline is rotated counterclockwise instead of clockwise as in figure 7(c). The resulting effect on the flow velocities are easily seen in figures 12(d) to (h). The rotation of the zero streamline relative to the wind in a counterclockwise direction is characteristic of many basins where the depth increases from the mainland shore to an interior point. For example reference 2 shows this effect for a rectangular basin without an island. As we found previously, the amount of rotation of the zero streamline depends on the depth of the basin and bottom topography slopes. The streamline patterns for $h/d = 0.5$ at the mainland and $h/d = 3.0$ at the island are shown in figures 13(c) and 14(c), respectively, for island diameters of 0.5 and 0.25. Near the islands, the zero streamline for these cases have been twisted counterclockwise considerably more than in the case shown in figure 12(c). This local increase in rotation is due to the large bottom slopes near the islands as shown in figures 13(a) and 14(a) as compared with the ones in figure 12(a).

Other cases noted in table I are also included for the interested reader but are not discussed.

CONCLUDING REMARKS

An analytical solution has been obtained for the wind-driven circulation in a shallow lake containing an island. The effect of an eccentric circular island in a circular lake where the bottom depth is decreasing from the mainland shore to the island is shown. This island effect is contrasted with the more usual case where the bottom depth increases from the mainland shore to some interior point. The island effect is shown to produce a completely different volume flow pattern (here the volume flow refers to the vertically integrated velocities). These volume flow patterns result in unusual velocity patterns that include the acceleration of flow near the island shore.

Lewis Research Center,
National Aeronautics and Space Administration,
Cleveland, Ohio, August 6, 1971,
129-01.

APPENDIX - SYMBOLS

A	function of h/d given by eq. (2)
a	mapping parameter defined by eq. (94)
B	function of h/d given by eq. (2)
C	function of h/d defined in eq. (5) or distance along mainland shore
$\mathscr{C}$	mainland shore line
C_o	contour of integration in T-plane
D	function of h/d defined in eq. (5)
d	Ekman friction depth, $\pi(2\nu/f_c)^{1/2}$
E	functions of h/d defined in eq. (6)
F	functions of h/d defined in eq. (13)
$\mathscr{F}$	defined by eq. (28)
f	function defined by eq. (22)
f_c	Coriolis parameter
g	acceleration due to gravity
H	defined in eq. (19)
H_o	value of H at lake or sea mainland shore
h	depth of lake or sea
I_n	defined in eq. (75)
$\mathscr{Im}$	imaginary part
J_n	defined in eq. (67)
$J_n^{(1)}, J_n^{(2)}$	defined in eq. (84)
K_n	defined by eq. (66)
$l_0, l_1, l_1^{(n)}, l_2^{(n)}$	constants of integration
$M_n(\zeta)$	constant defined in eq. (92)
n	integer
$\hat{n}$	unit normal to boundary of sea or lake
n_1, n_2	x- and y-components of $\hat{n}$
p_o, q_o, p_s, q_s	constants defined in eq. (34)

Q	$Q_1 + iQ_2 = \frac{\partial\psi}{\partial y} - i\frac{\partial\psi}{\partial x}$
Q_1, Q_2	x- and y-components of volume flow
R_o	radius of outer circle in T-plane
$\mathcal{R}e$	real part
$\mathcal{R}es$	residue
r	radius of mainland shore for circular lake
r_s	radius of circular island
S	distance along island shore line
$\mathcal{S}$	island shore line
s_o, s_s	constants defined in eq. (34)
T	e^w
t	dummy variable of integration
U	x-component of horizontal velocity
u	harmonic function of x and y
u_s	u-coordinate of boundary of rectangle in w-plane
V	y-component of horizontal velocity
v	harmonic conjugate of u
w	complex function $u + iv$
x	coordinate of lake surface plane
x_a, x_b	x-coordinates of island boundary points
y	coordinate of lake surface plane
Z	transformed dependent variable
z	$x + iy$
α, β	defined in eq. (21)
$\Gamma_n(u), \gamma_n(u)$	Fourier coefficients defined in eq. (44)
δ	parameter in depth distribution, eq. (53)
ζ	displacement of sea or lake surface
η	dummy variable
λ_n	eigenvalue defined in eq. (64)
ν	coefficient of vertical eddy diffusivity

ξ	vertical distance measured upwards from water surface
σ	$\sigma^{(1)} + i\sigma^{(2)}$
$\sigma^{(1)}, \sigma^{(2)}$	defined in terms of wind stress by eq. (9)
τ^{w}	$\tau_1^{w} + i\tau_2^{w}$
τ_1^{w}, τ_2^{w}	x, y components of wind stress divided by density
ψ	stream function for the volume flow Q
Ω_n	Fourier coefficient defined by eq. (41)
$\Omega_n^{(0)}, \Omega_n^{(1)}, \Omega_n^{(2)}$	defined by eqs. (85) and (91)
$\omega_n(u; \zeta)$	defined in eq. (68)

Subscripts:

u, v	partial derivative
x, y	partial derivative

Superscript:

*	denotes complex conjugate

REFERENCES

1. Welander, Pierre: Wind Action on a Shallow Sea: Some Generalizations of Ekman's Theory. Tellus, vol. 9, no. 1, Feb. 1957, pp. 45-52.
2. Gedney, Richard T.: Numerical Calculations of the Wind-Driven Currents in Lake Erie. Ph. D. thesis, Case-Western Reserve University, 1971.
3. Goldstein, Marvin E.; Braun, Willis, H.; and Gedney, Richard T.: A Method for Obtaining Analytical Solutions to the Equation for Wind-Driven Circulation in a Shallow Sea or Lake. NASA TN D-5989, 1970.
4. Churchill, Ruel V.: Complex Variables and Applications. Second ed., Mc-Graw-Hill Book Co., Inc., 1960.

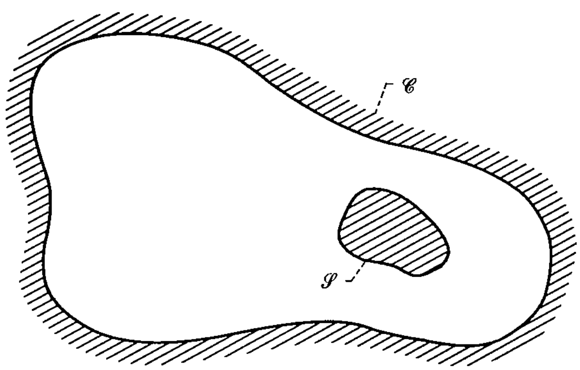

Figure 1. - Lake (sea) - island configuration.

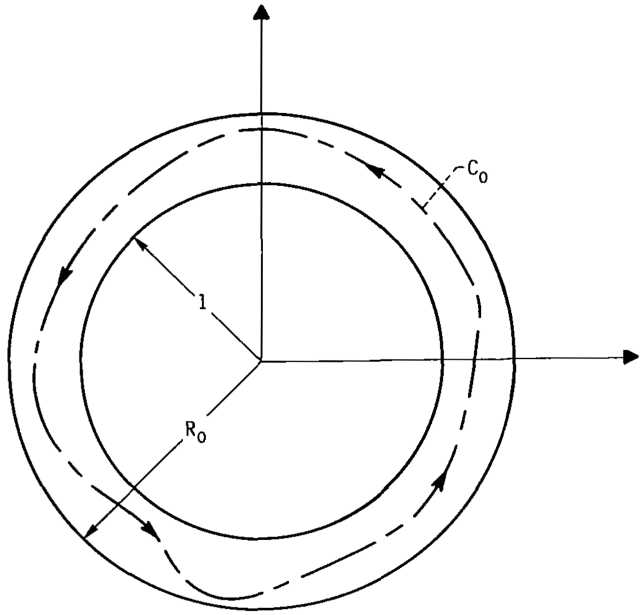

Figure 2. - Annular region in T-plane.

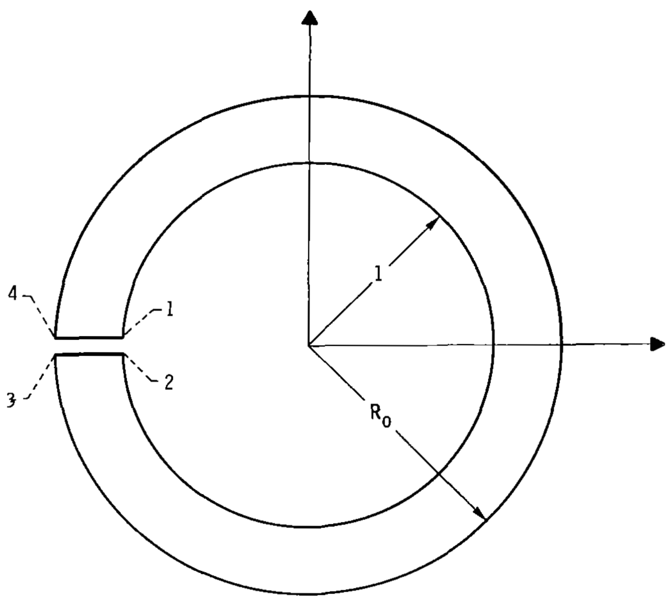

Figure 3. - Cut annular region in T-plane.

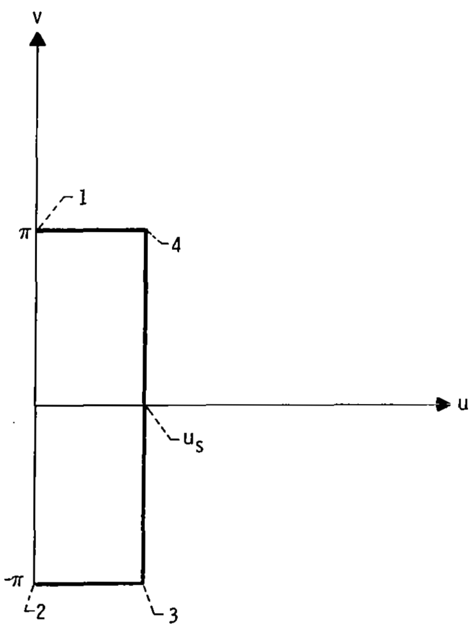

Figure 4. - Rectangular region in W-plane.

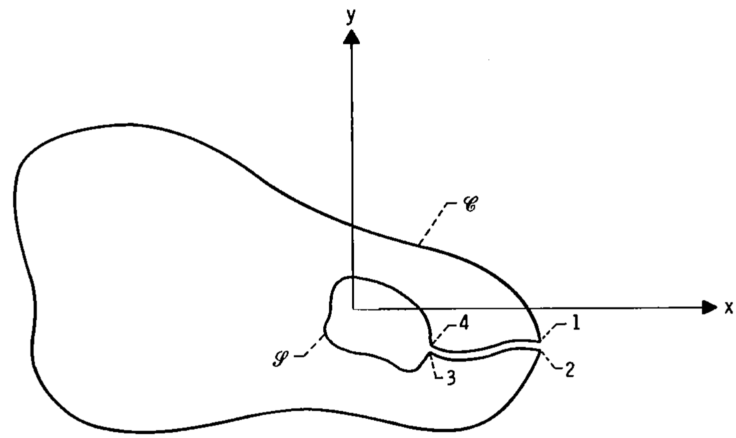

Figure 5. - Cut lake (sea) configuration.

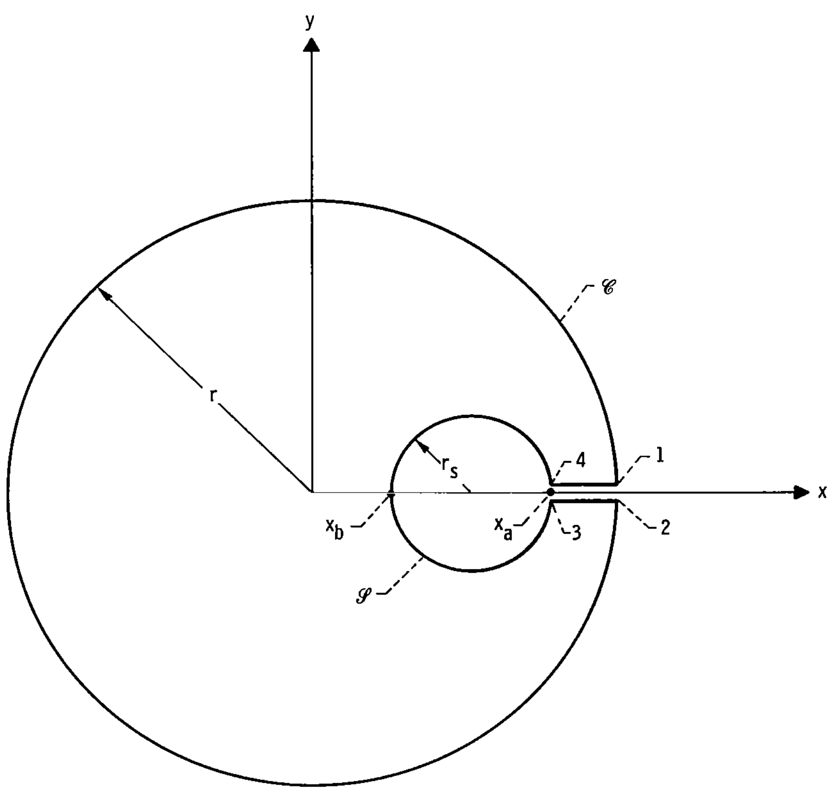

Figure 6. - Circular lake and island configuration.

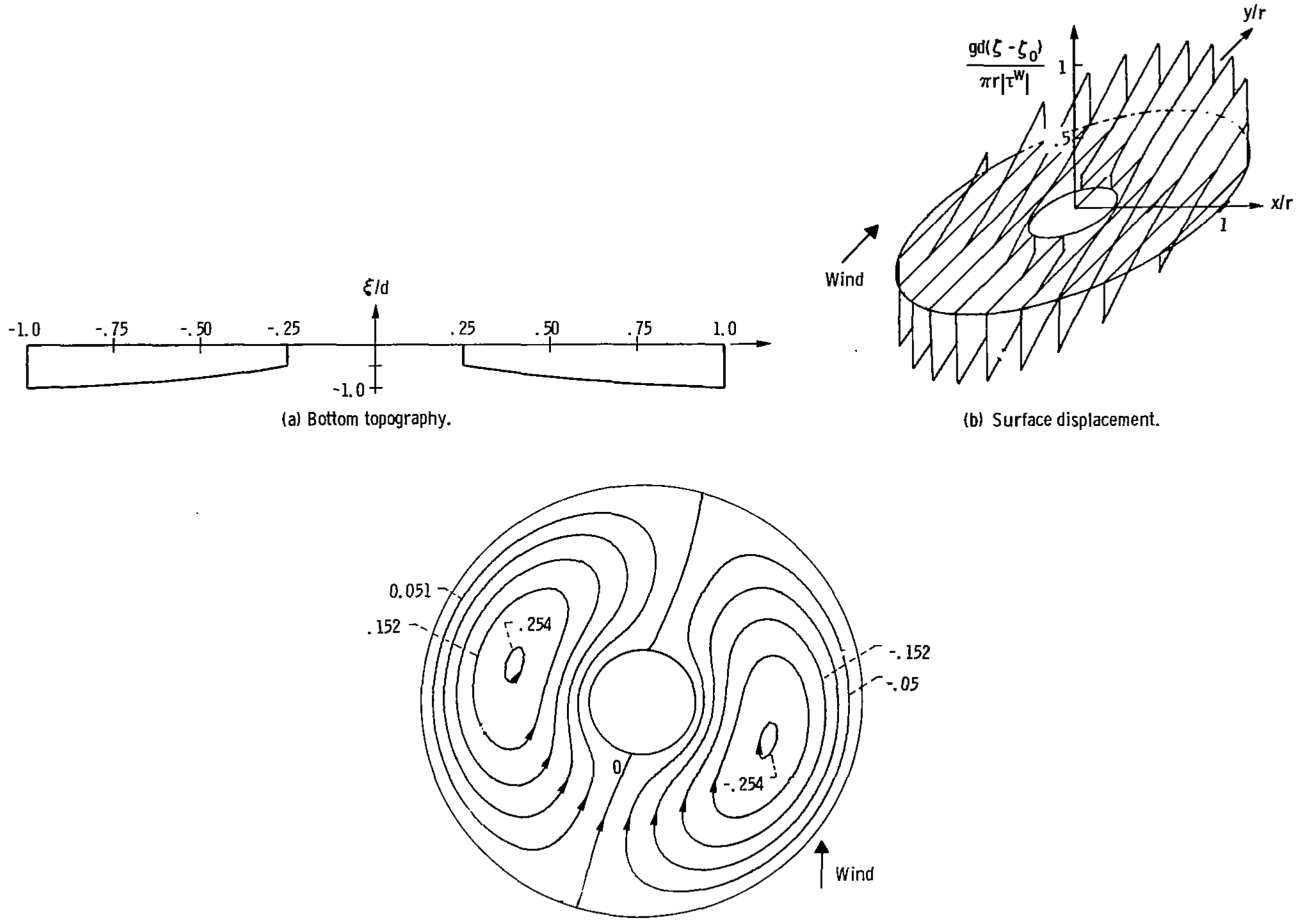

(a) Bottom topography.

(b) Surface displacement.

(c) Nondimensional stream function $2\pi f_c\,\psi/|\tau^W|$.

Figure 7. - Circular basin circulation. Island eccentricity = 0; island diameter = 0.5; h/d = 1.0 at mainland shore; h/d = 0.5 at island; $\tau^W/|\tau^W|$ = i.

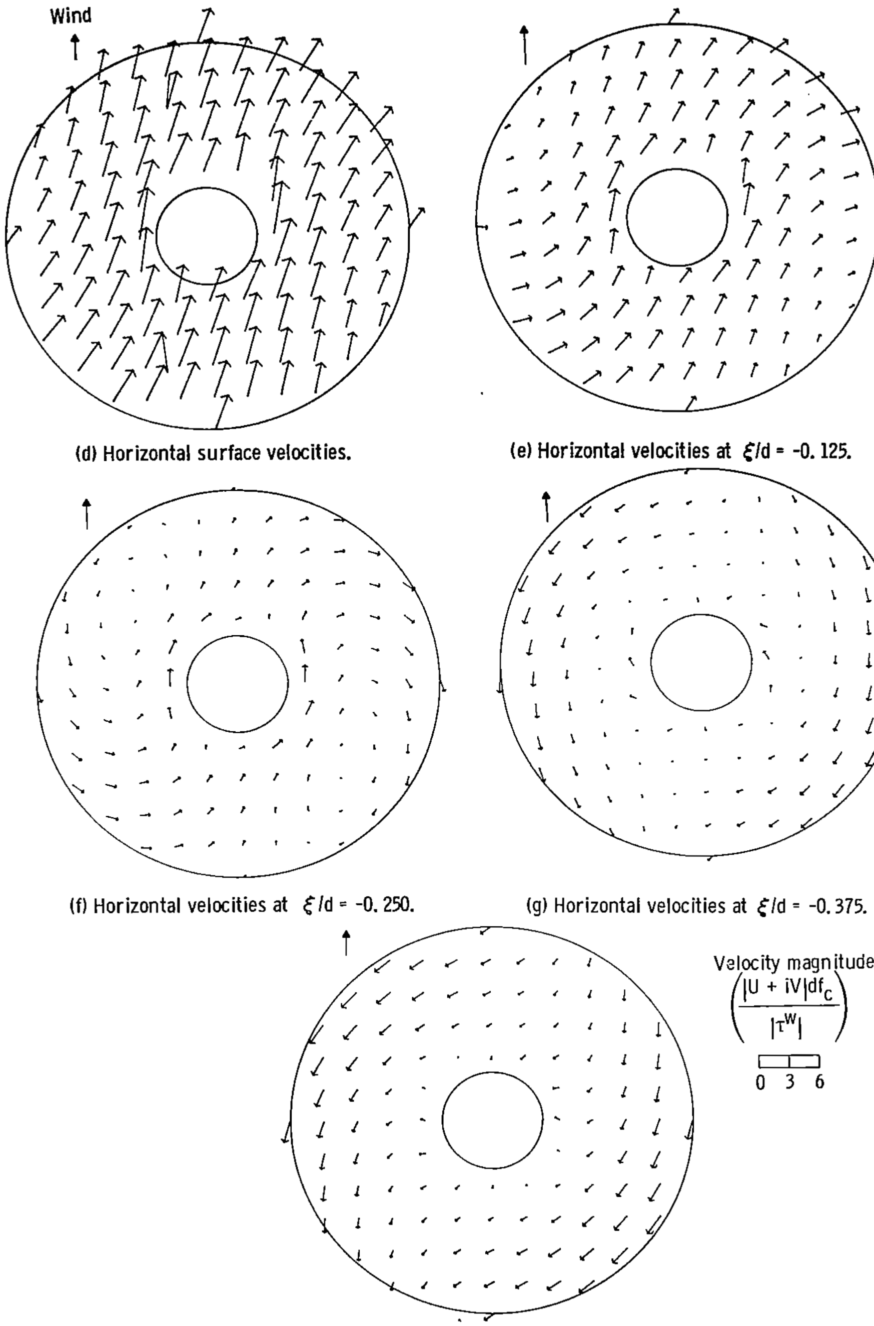

(d) Horizontal surface velocities.

(e) Horizontal velocities at $\xi/d = -0.125$.

(f) Horizontal velocities at $\xi/d = -0.250$.

(g) Horizontal velocities at $\xi/d = -0.375$.

(h) Horizontal velocities at $\xi/d = -0.500$.

Figure 7. - Concluded.

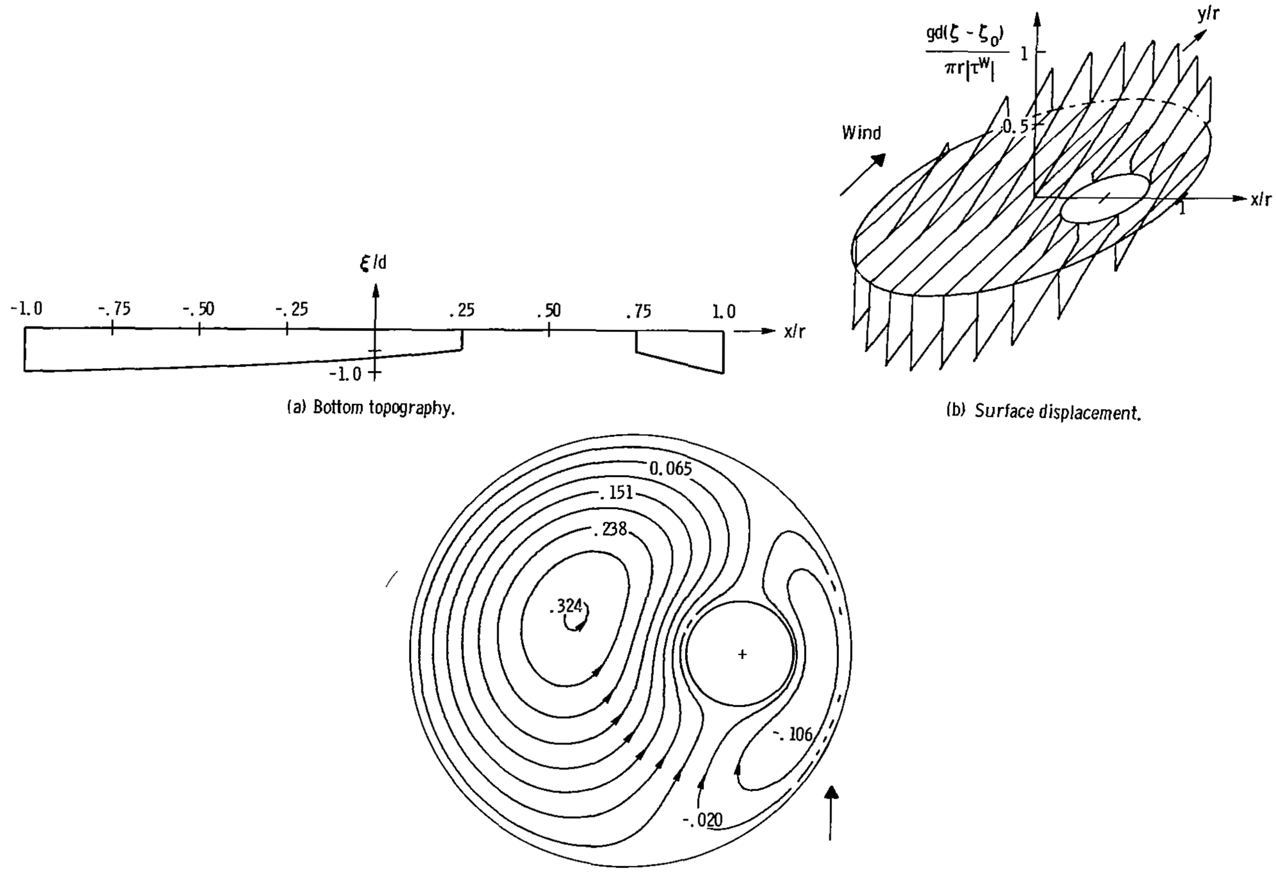

(a) Bottom topography.

(b) Surface displacement.

(c) Nondimensional stream function $2\pi f_c \psi / |\tau^W|$.

Figure 8. - Circular basin circulation. Island eccentricity = 0.5 island diameter = 0.5; h/d = 1.0 at mainland shore; h/d = 0.5 at island; $\tau^W/|\tau^W| = i$.

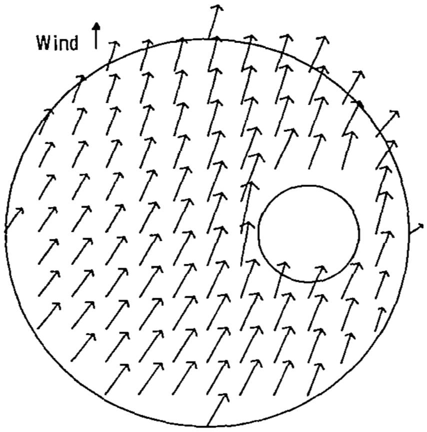

(d) Horizontal surface velocities.

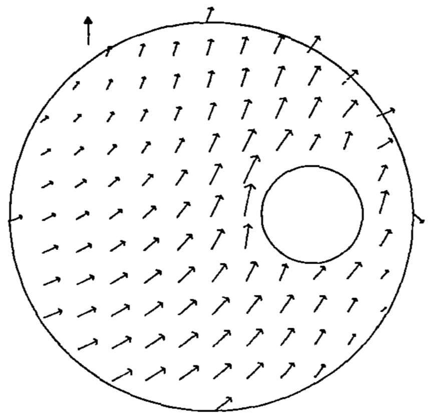

(e) Horizontal velocities at $\xi/d = -0.125$.

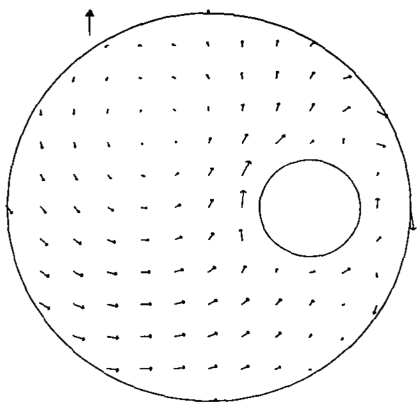

(f) Horizontal velocities at $\xi/d = -0.250$.

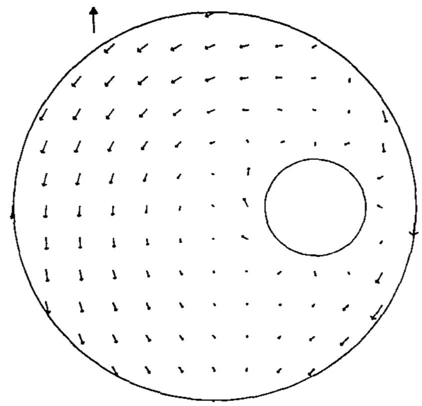

(g) Horizontal velocities at $\xi/d = -0.375$.

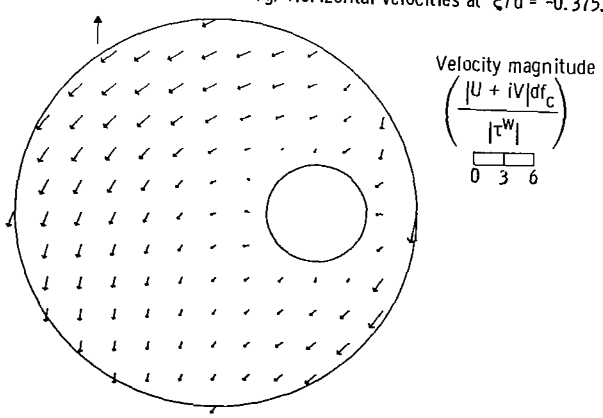

(h) Horizontal velocities at $\xi/d = -0.500$.

Figure 8. - Concluded.

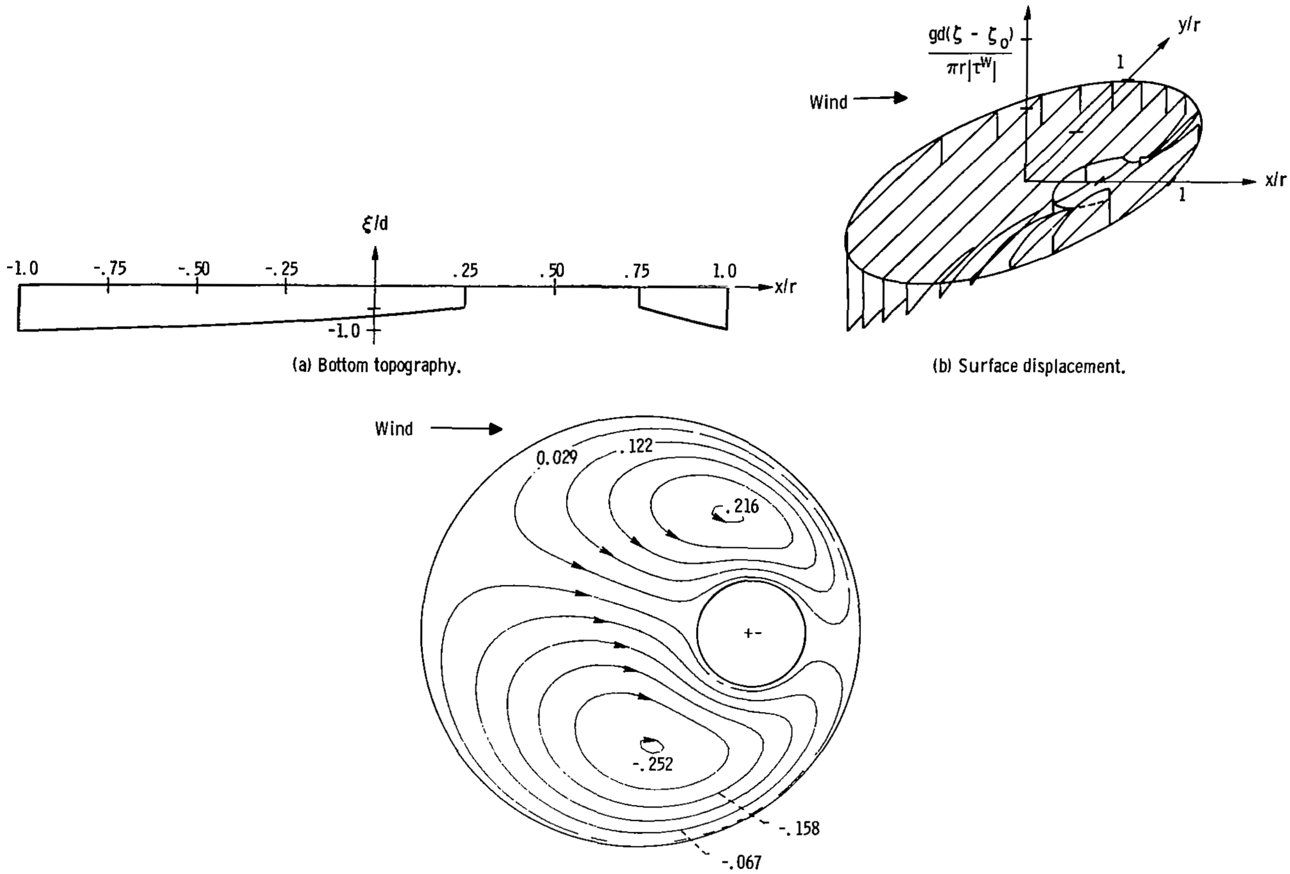

(a) Bottom topography.

(b) Surface displacement.

(c) Nondimensional stream function $2\pi f_c \psi / |\tau^W|$.

Figure 9. - Circular basin circulation. Island eccentricity = 0.5; island diameter = 0.5; h/d = 1.0 at mainland shore; h/d = 0.5 at island; $\tau^W/|\tau^W|$ = 1.0.

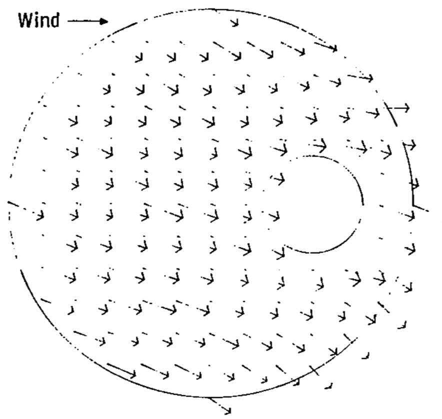

(d) Horizontal velocities at ξ/d = -0.125.

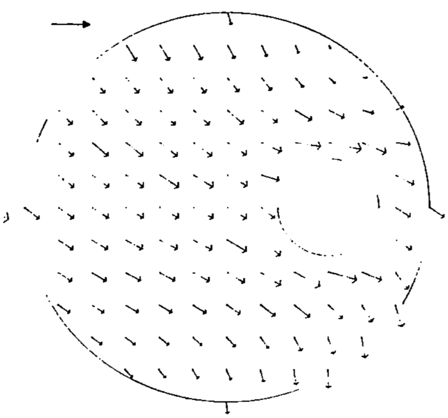

(e) Horizontal velocities at ξ/d = -0.250.

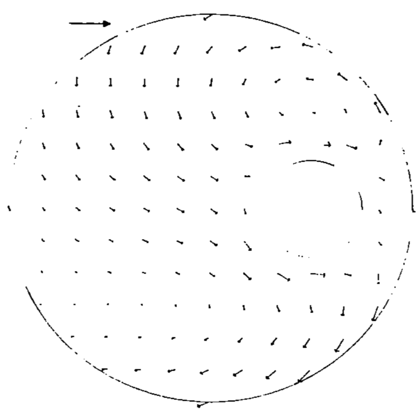

(f) Horizontal velocities at ξ/d = -0.250.

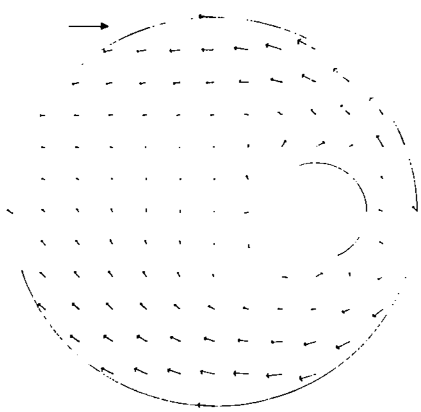

(g) Horizontal velocities at ξ/d = -0.275.

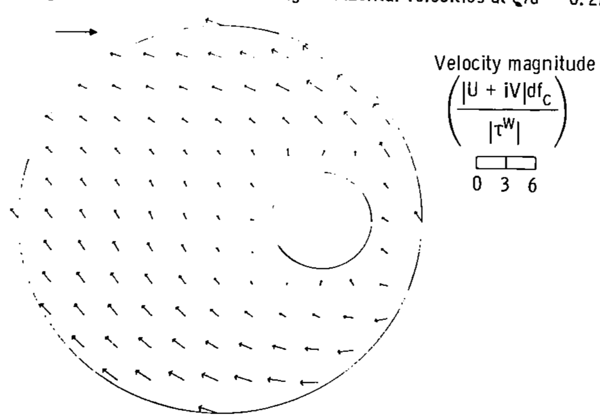

(h) Horizontal velocities at ξ/d = -0.500.

Figure 9. - Concluded.

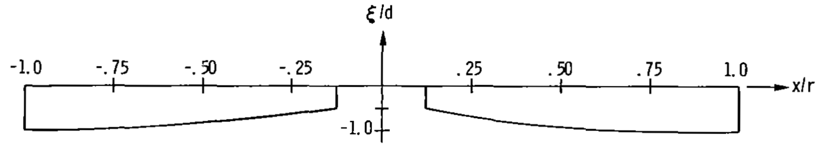

(a) Bottom topography.

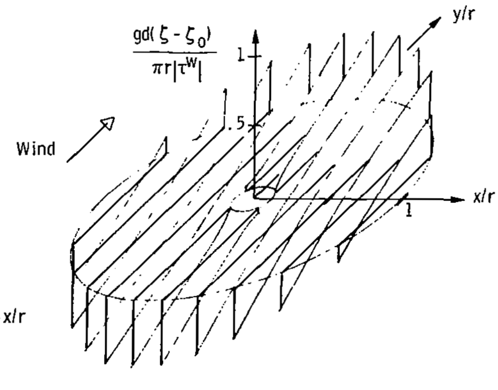

(b) Surface displacement.

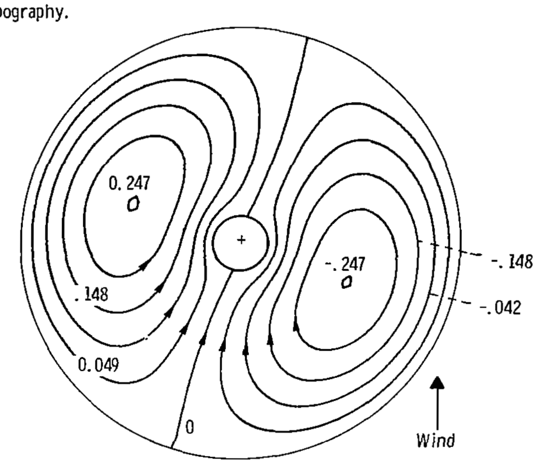

(c) Nondimensional stream function $2\pi f_c \psi / |\tau^W|$.

Figure 10. - Circular basin circulation. Island eccentricity = 0; island diameter = 0.25; h/d = 1.0 at mainland shore; h/d = 0.5 at island; $\tau^W/|\tau^W| = i$.

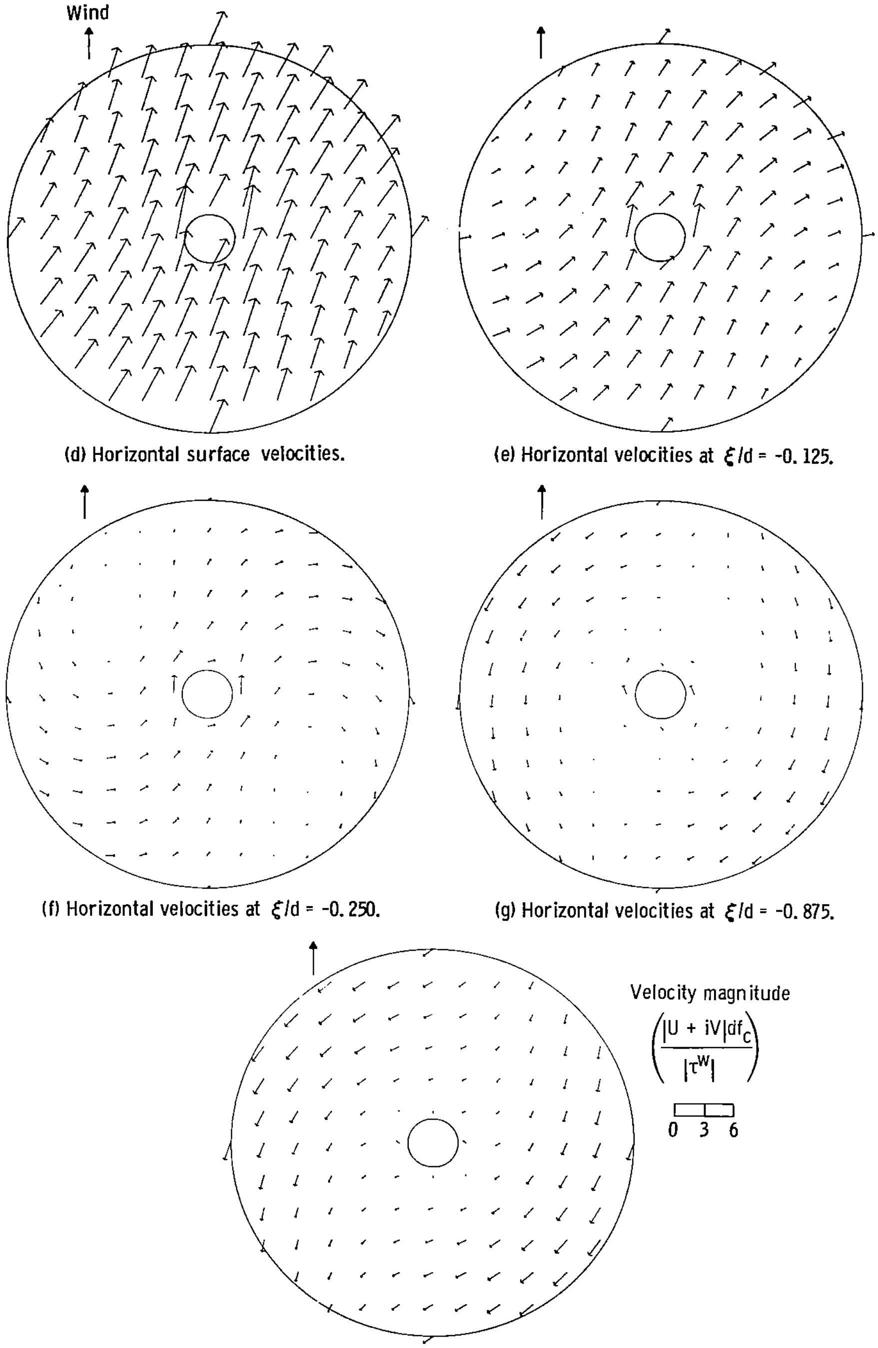

(d) Horizontal surface velocities.

(e) Horizontal velocities at ξ/d = -0.125.

(f) Horizontal velocities at ξ/d = -0.250.

(g) Horizontal velocities at ξ/d = -0.875.

(h) Horizontal velocities at ξ/d = -0.500.

Figure 10. - Concluded.

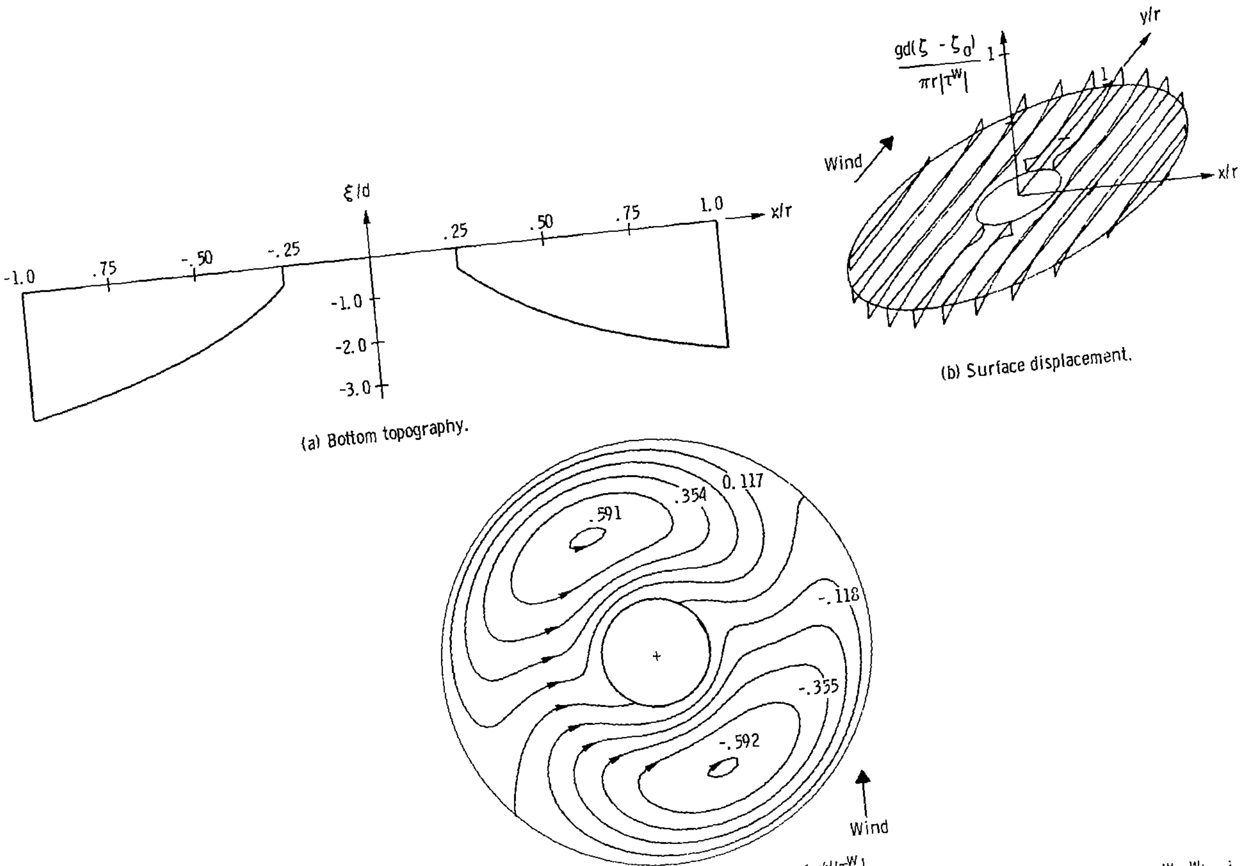

(a) Bottom topography.

(b) Surface displacement.

(c) Nondimensional stream function $2\pi i_c \psi/|\tau^W|$.

Figure 11. - Circular basin circulation. Island eccentricity = 0; island diameter = 0.5; h/d = 3.0 at mainland shore; h/d = 0.5 at island; $\tau^W/|\tau^W|$ = i.

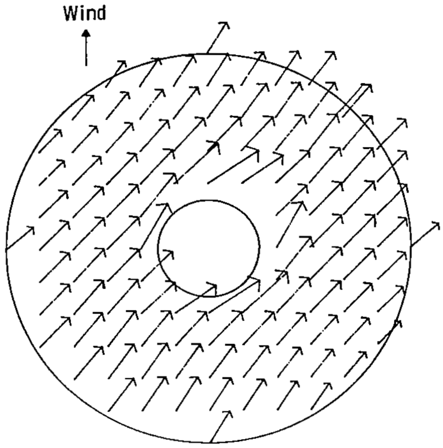

(d) Horizontal surface velocities.

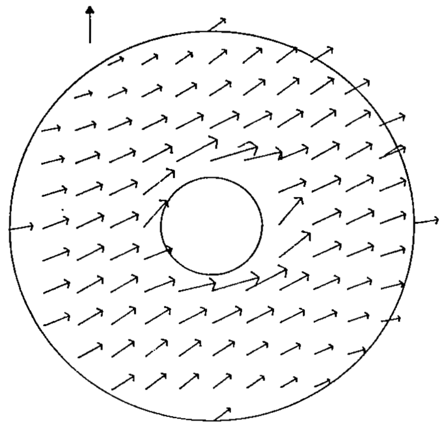

(e) Horizontal velocities at $\xi/d = -0.125$.

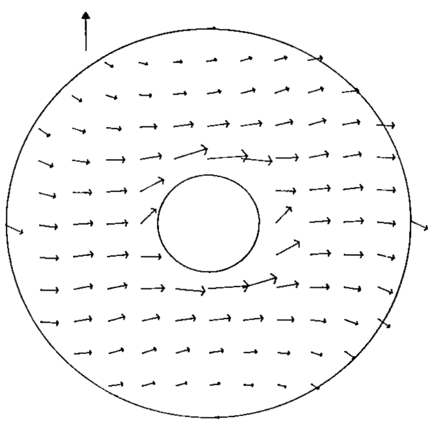

(f) Horizontal velocities at $\xi/d = -0.250$.

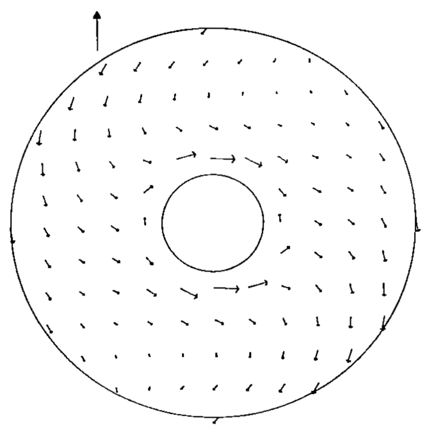

(g) Horizontal velocities at $\xi/d = -0.500$.

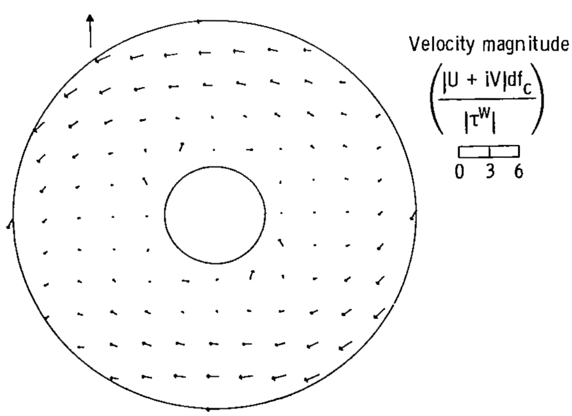

(h) Horizontal velocities at $\xi/d = -1.000$.

Figure 11. - Concluded.

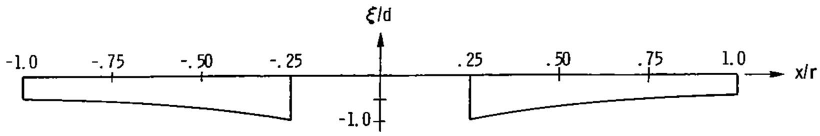

(a) Bottom topography.

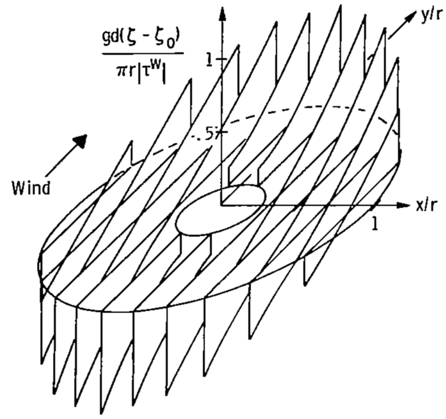

(b) Surface displacement.

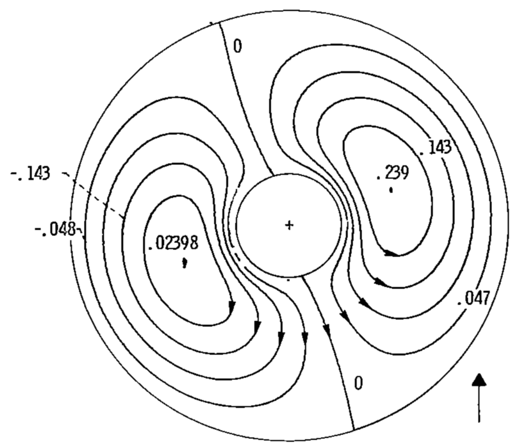

(c) Nondimensional stream function $2\pi f_c \psi/|\tau^W|$.

Figure 12. - Circular basin circulation. Island eccentricity = 0; island diameter = 0.5; h/d = 0.5 at mainland shore; h/d = 1.0 at island; $\tau^W/|\tau^W| = i$.

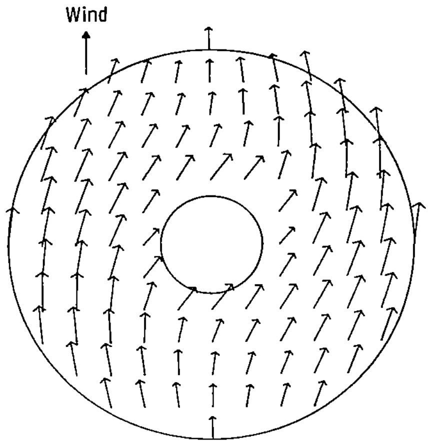

(d) Horizontal surface velocities.

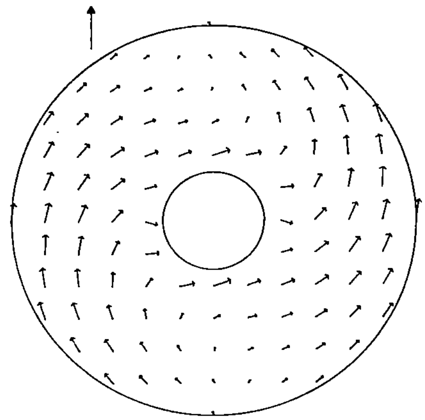

(e) Horizontal velocities at ξ/d = -0.125.

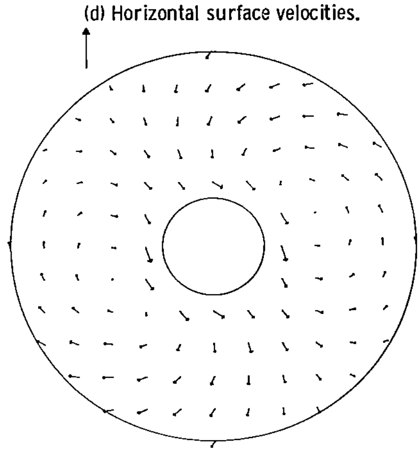

(f) Horizontal velocities at ξ/d = -0.250.

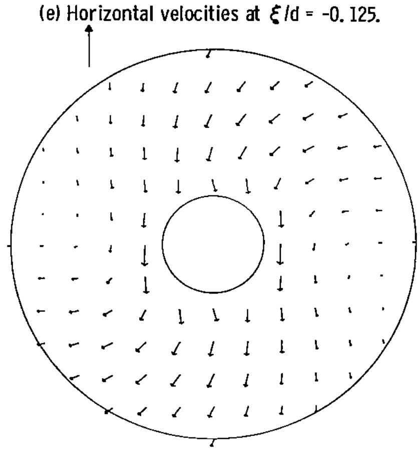

(g) Horizontal velocities at ξ/d = -0.375.

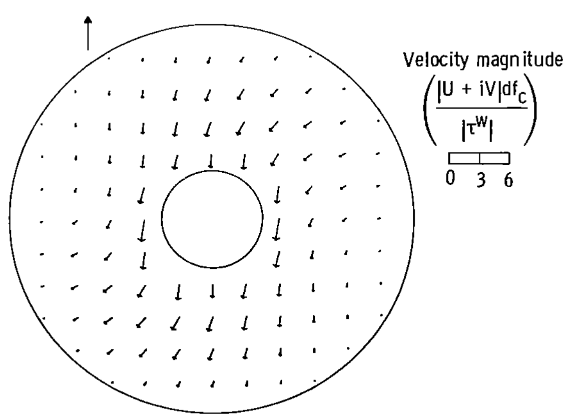

(h) Horizontal velocities at ξ/d = -0.500.

Figure 12. - Concluded.

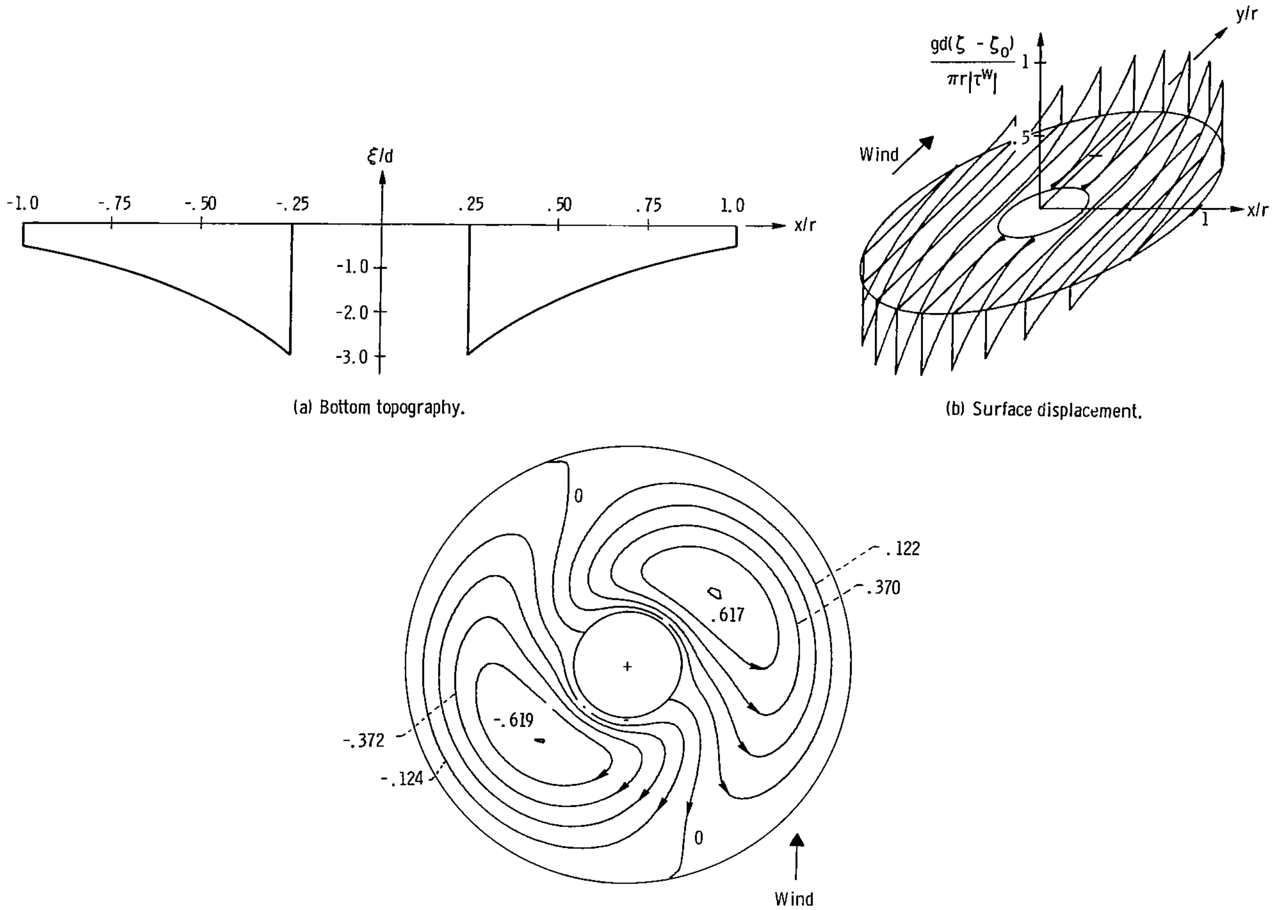

(c) Nondimensional stream function $2\pi f_c \psi/|\tau^W|$.

Figure 13. - Circular basin circulation. Island eccentricity = 0; island diameter = 0.5; h/d = 0.5 at mainland shore; h/d = 3.0 at island; $\tau^W/|\tau^W| = i$.

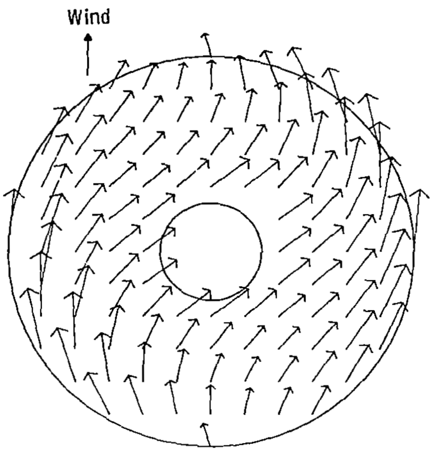

(d) Horizontal surface velocities.

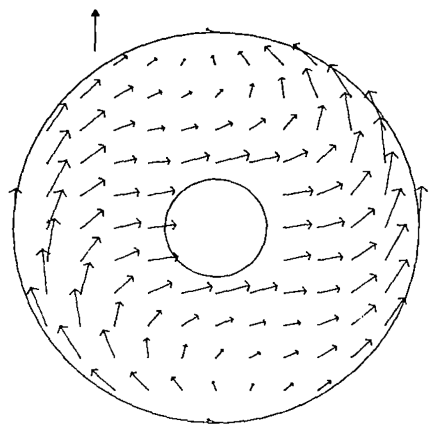

(e) Horizontal velocities at ξ/d = -0.125.

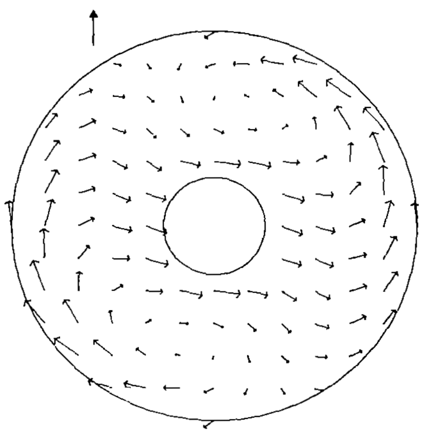

(f) Horizontal velocities at ξ/d = -0.250.

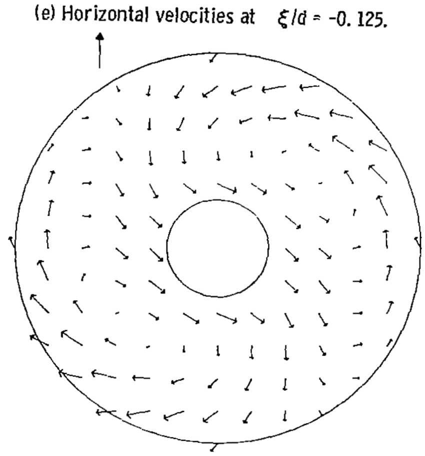

(g) Horizontal velocities at ξ/d = -0.375.

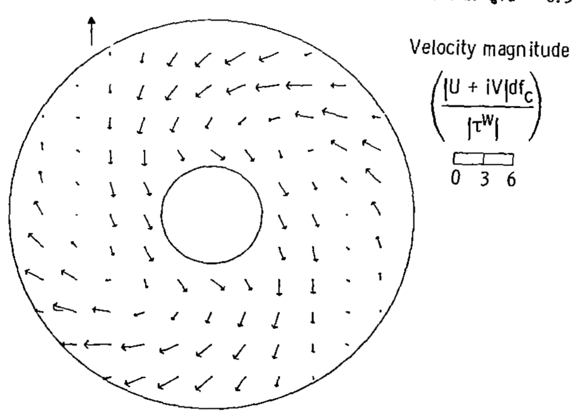

(h) Horizontal velocities at ξ/d = -0.500.

Figure 13. - Concluded.

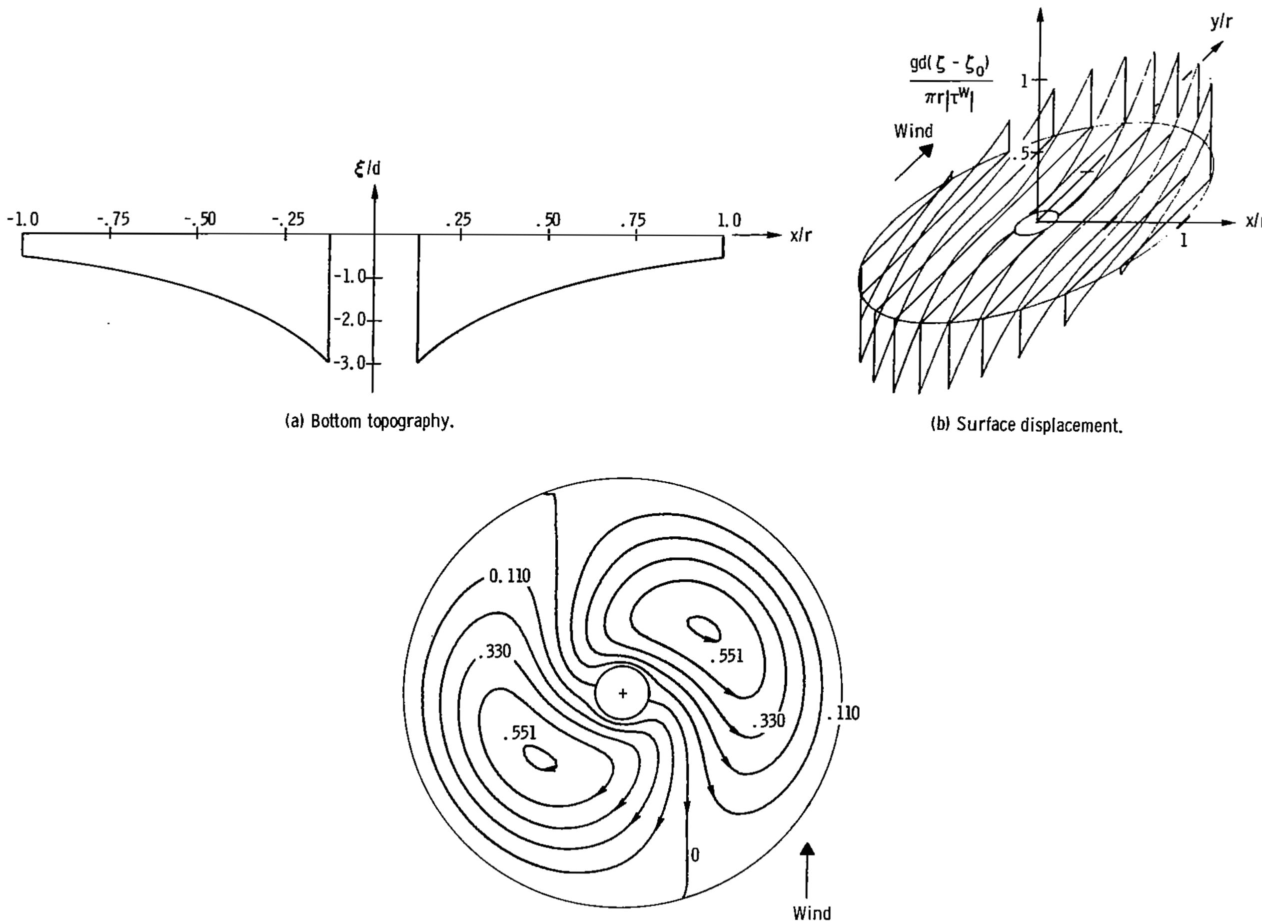

(a) Bottom topography.

(b) Surface displacement.

(c) Nondimensional stream function $2\pi f_c \psi / |\tau^W|$.

Figure 14. - Circular basin circulation. Island eccentricity = 0; island diameter = 0.25; h/d = 0.5 at mainland shore; h/d = 3.0 at island; $\tau^W / |\tau^W| = i$.

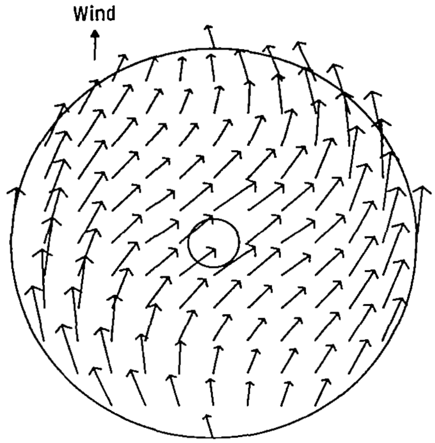

(d) Horizontal surface velocities.

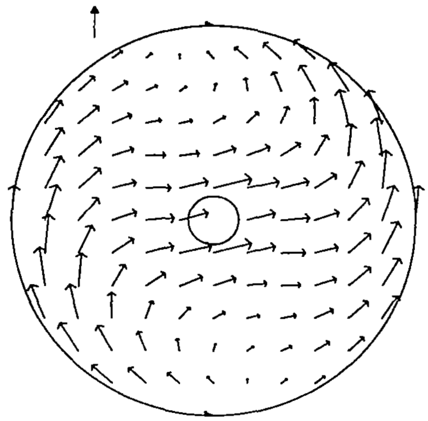

(e) Horizontal velocities at ξ/d = -0.125.

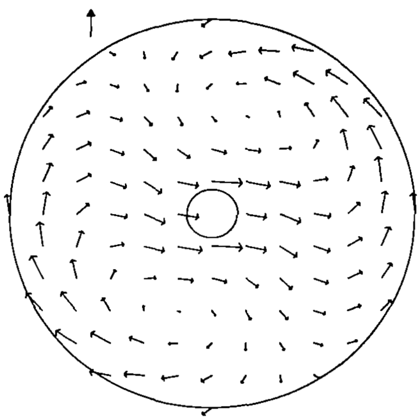

(f) Horizontal velocities at ξ/d = -0.250.

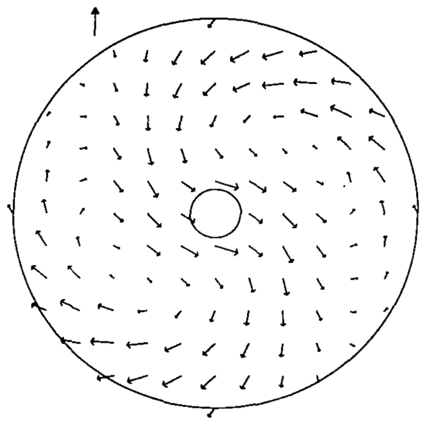

(g) Horizontal velocities at ξ/d = -0.375.

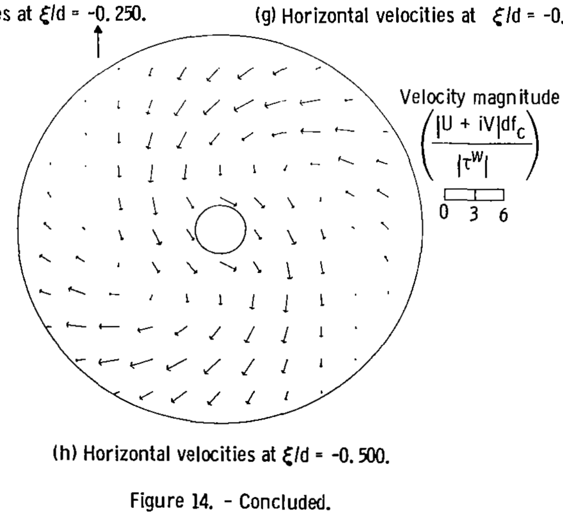

(h) Horizontal velocities at ξ/d = -0.500.

Figure 14. - Concluded.

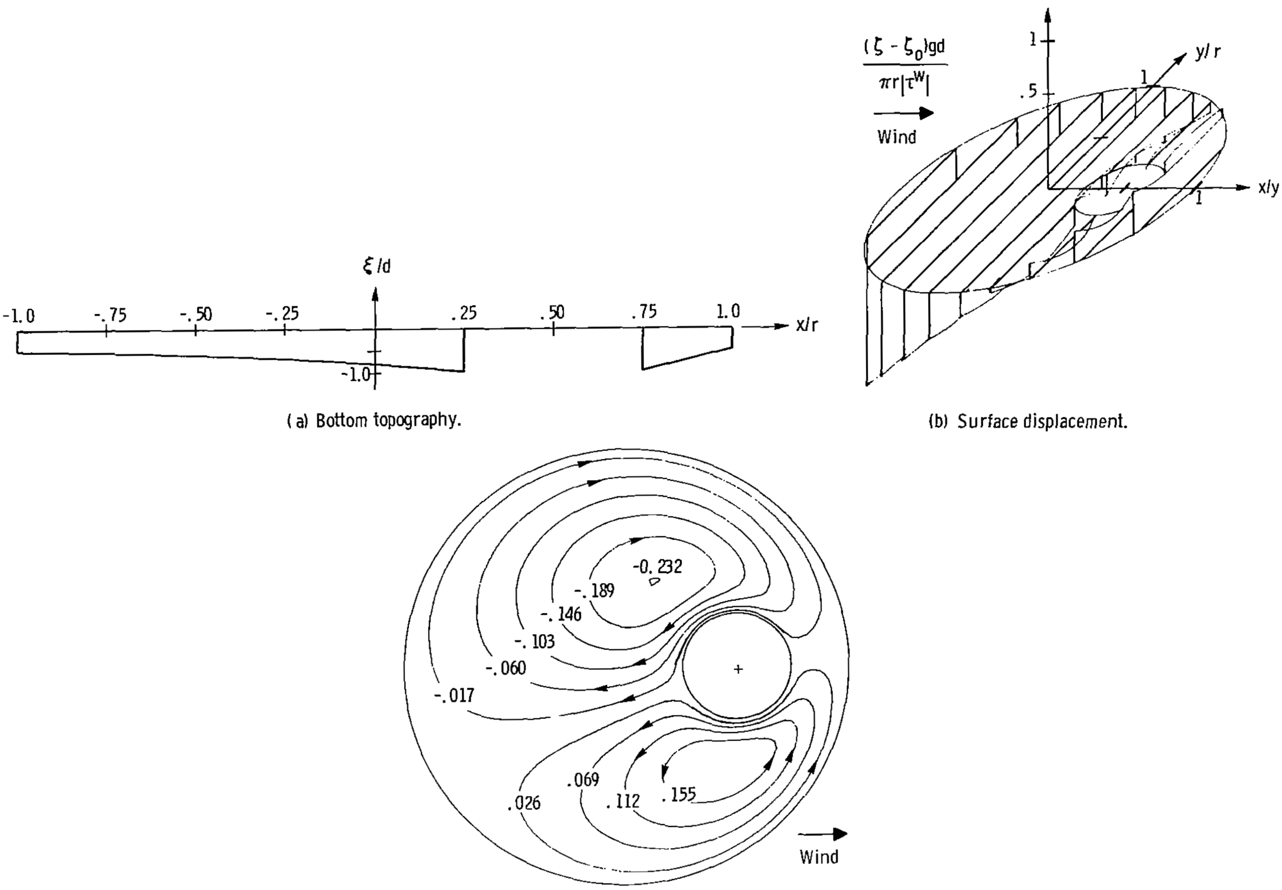

(a) Bottom topography.

(b) Surface displacement.

(c) Nondimensional stream function $2\pi f_c \psi/|\tau^W|$.

Figure 15. - Circular basin circulation. Island eccentricity = 0.5; island diameter = 0.5; h/d = 0.5 at mainland shore; h/d = 1.0 at island; $\tau^W/|\tau^W|$ = 1.0.

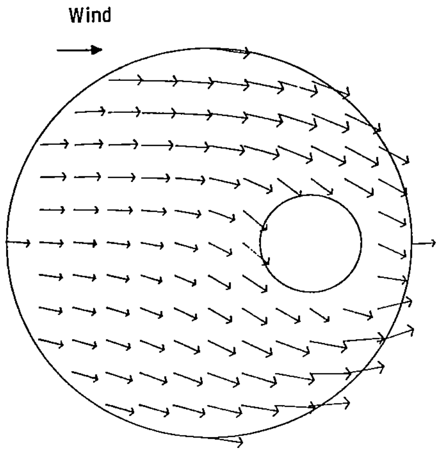

(d) Horizontal surface velocities.

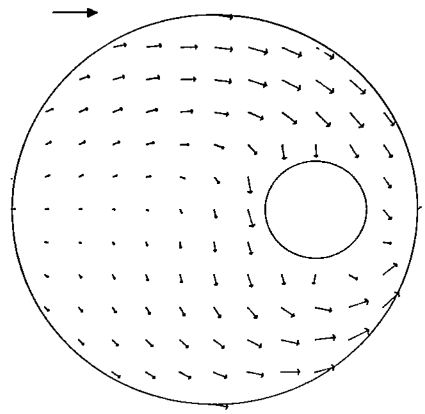

(e) Horizontal velocities at $\xi/d = -0.125$.

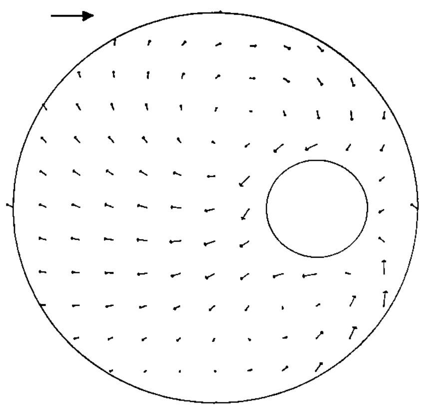

(f) Horizontal velocities at $\xi/d = -0.250$.

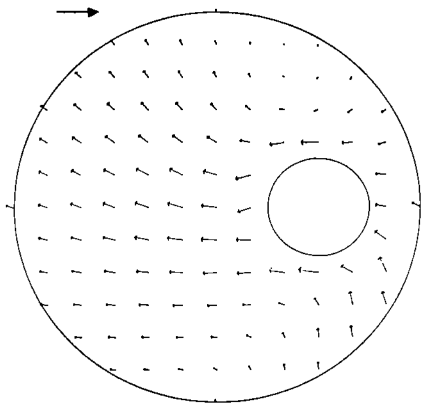

(g) Horizontal velocities at $\xi/d = -0.375$.

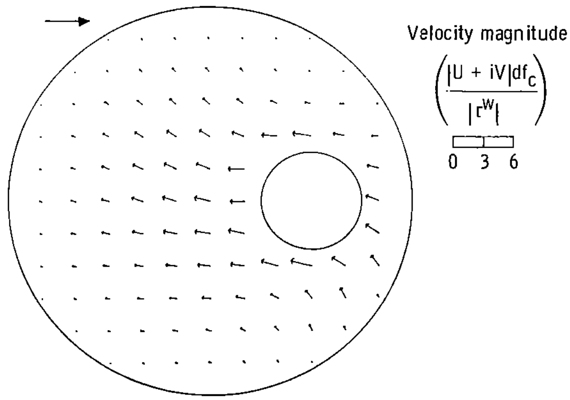

(h) Horizontal velocities at $\xi/d = -0.500$.

Figure 15. - Concluded.

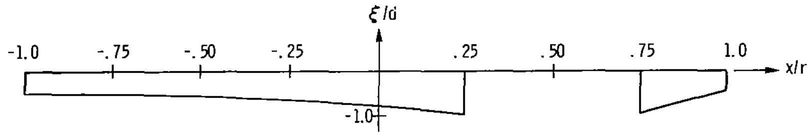

(a) Bottom topography.

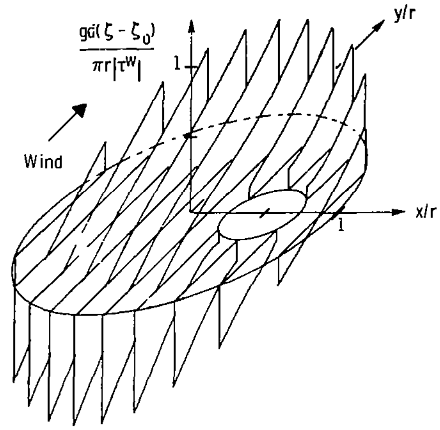

(b) Surface displacement.

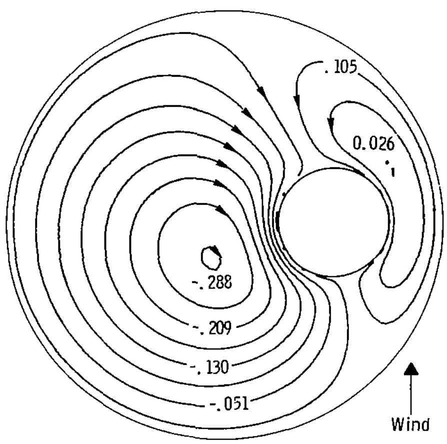

(c) Nondimensional stream function $2\pi f_c \psi / |\tau^W|$.

Figure 16. - Circular basin circulation. Island eccentricity = 0.5; island diameter = 0.5; h/d = 0.5 at mainland shore; h/d = 1.0 at island; $\tau^W/|\tau^W| = i$.

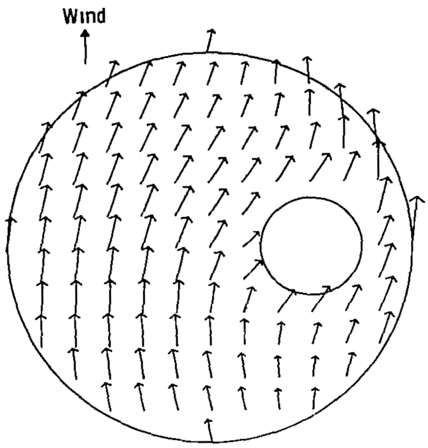

(d) Horizontal surface velocities.

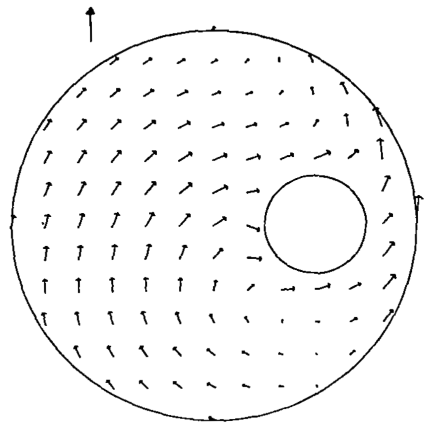

(e) Horizontal velocities at $\xi/d = -0.125$.

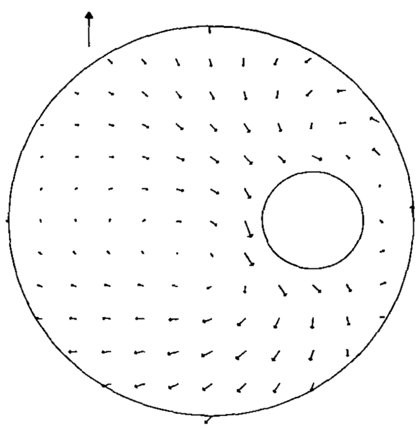

(f) Horizontal velocities at $\xi/d = -0.250$.

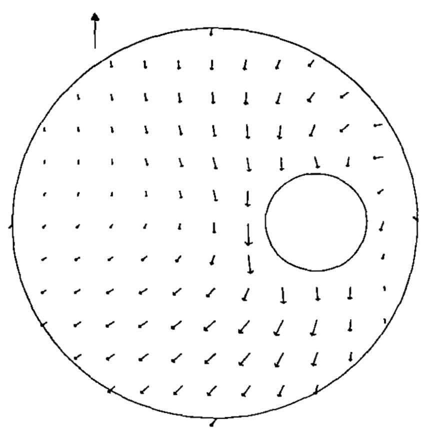

(g) Horizontal velocities at $\xi/d = -0.375$.

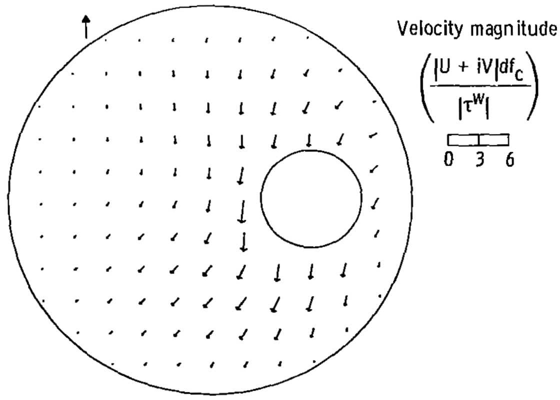

(h) Horizontal velocities at $\xi/d = -0.500$.

Figure 16. - Concluded.

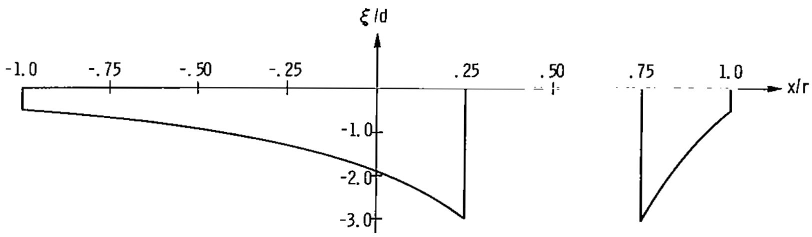

(a) Bottom topography.

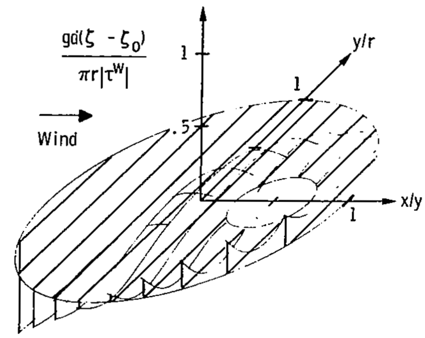

(b) Surface displacement.

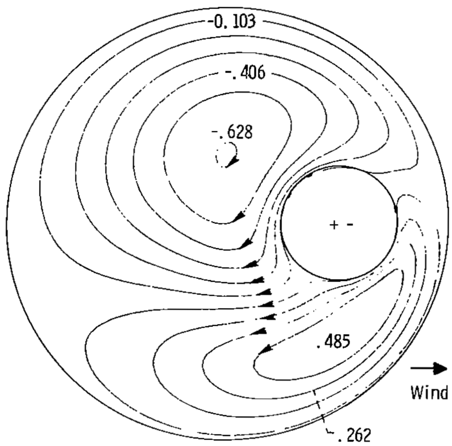

(c) Nondimensional stream function $2\pi f_c \psi/|\tau^W|$.

Figure 17. - Circular basin circulation. Island eccentricity = 0.5; island diameter = 0.5; h/d = 0.5 at mainland shore; h/d = 3.0 at island; $\tau^W/|\tau^W|$ = 1.0.

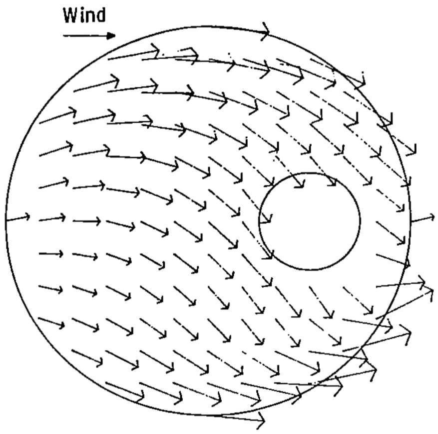

(d) Horizontal surface velocities.

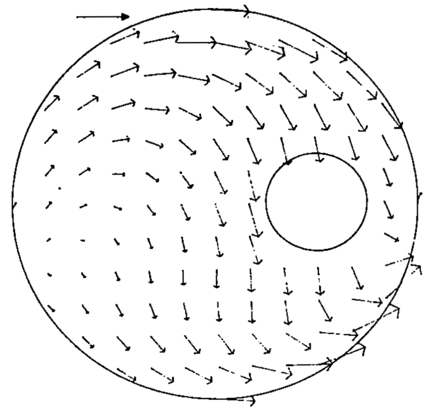

(e) Horizontal velocities at ξ/d = -0.125.

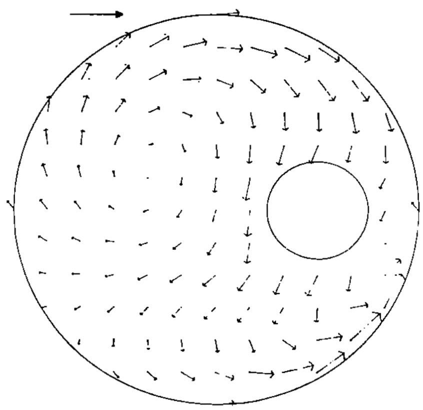

(f) Horizontal velocities at ξ/d = -0.250.

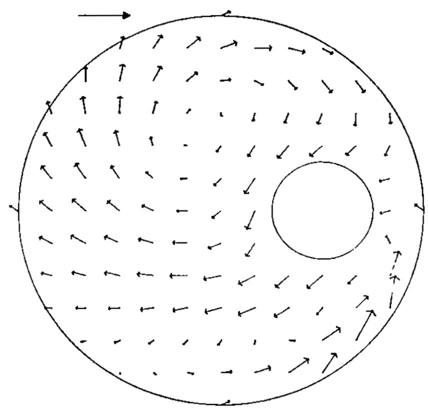

(g) Horizontal velocities at ξ/d = -0.375.

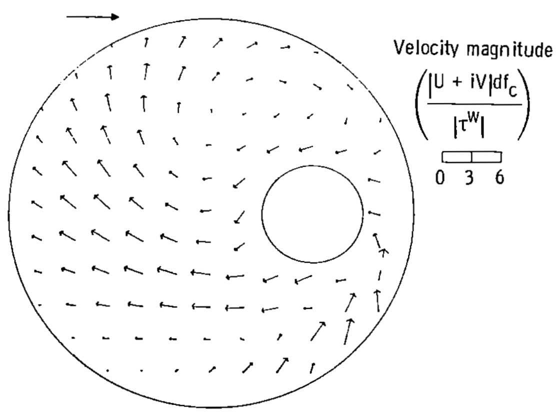

(h) Horizontal velocities at ξ/d = -0.500.

Figure 17. - Concluded.

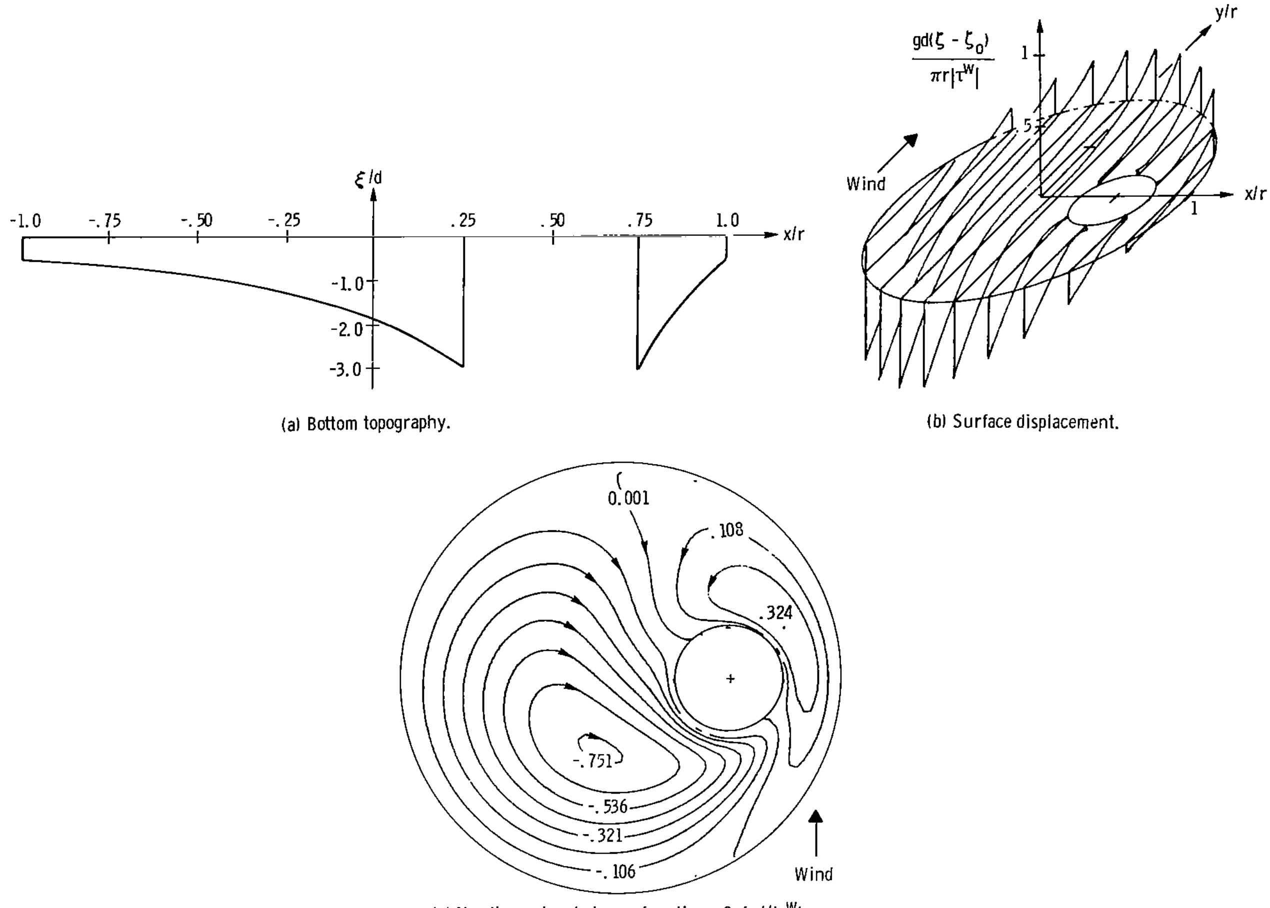

(a) Bottom topography.

(b) Surface displacement.

(c) Nondimensional stream function $2\pi f_c \psi / |\tau^W|$.

Figure 18. - Circular basin circulation. Island eccentricity = 0.5; island diameter = 0.5; h/d = 0.5 at mainland shore; h/d = 3.0 at island; $\tau^W/|\tau^W|$ = i.

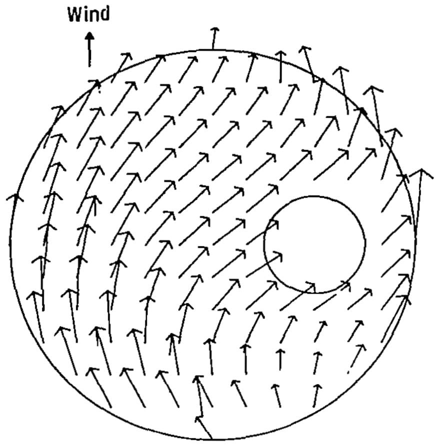

(d) Horizontal surface velocities.

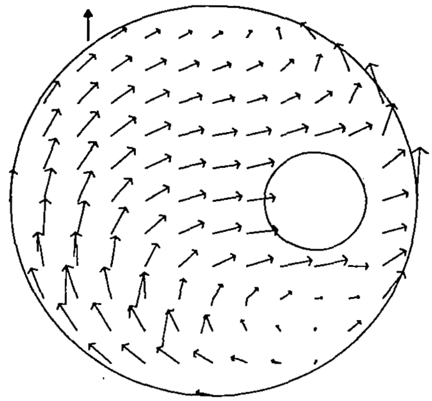

(e) Horizontal velocities at ξ/d = -0.125.

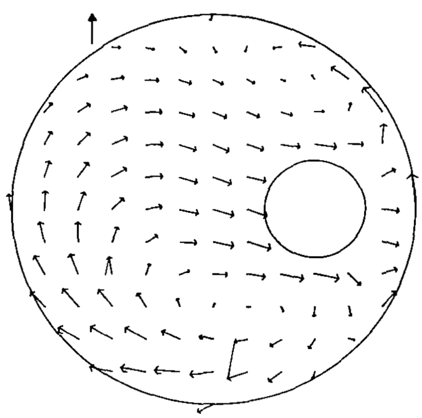

(f) Horizontal velocities at ξ/d = -0.250.

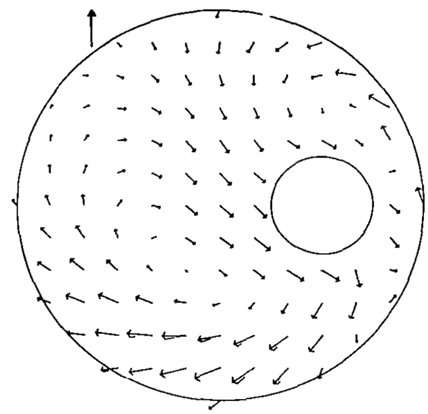

(g) Horizontal velocities at ξ/d = -0.375.

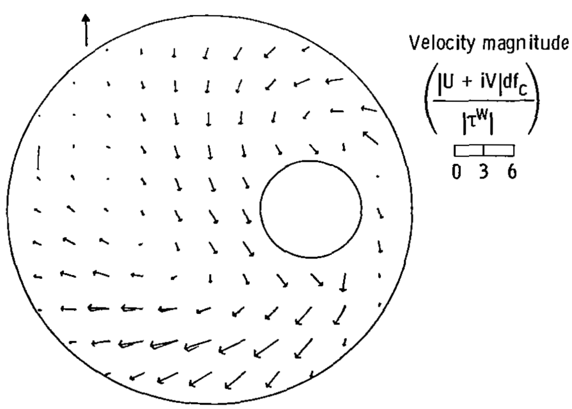

(h) Horizontal velocities at ξ/d = -0.500.

Figure 18. - Concluded.

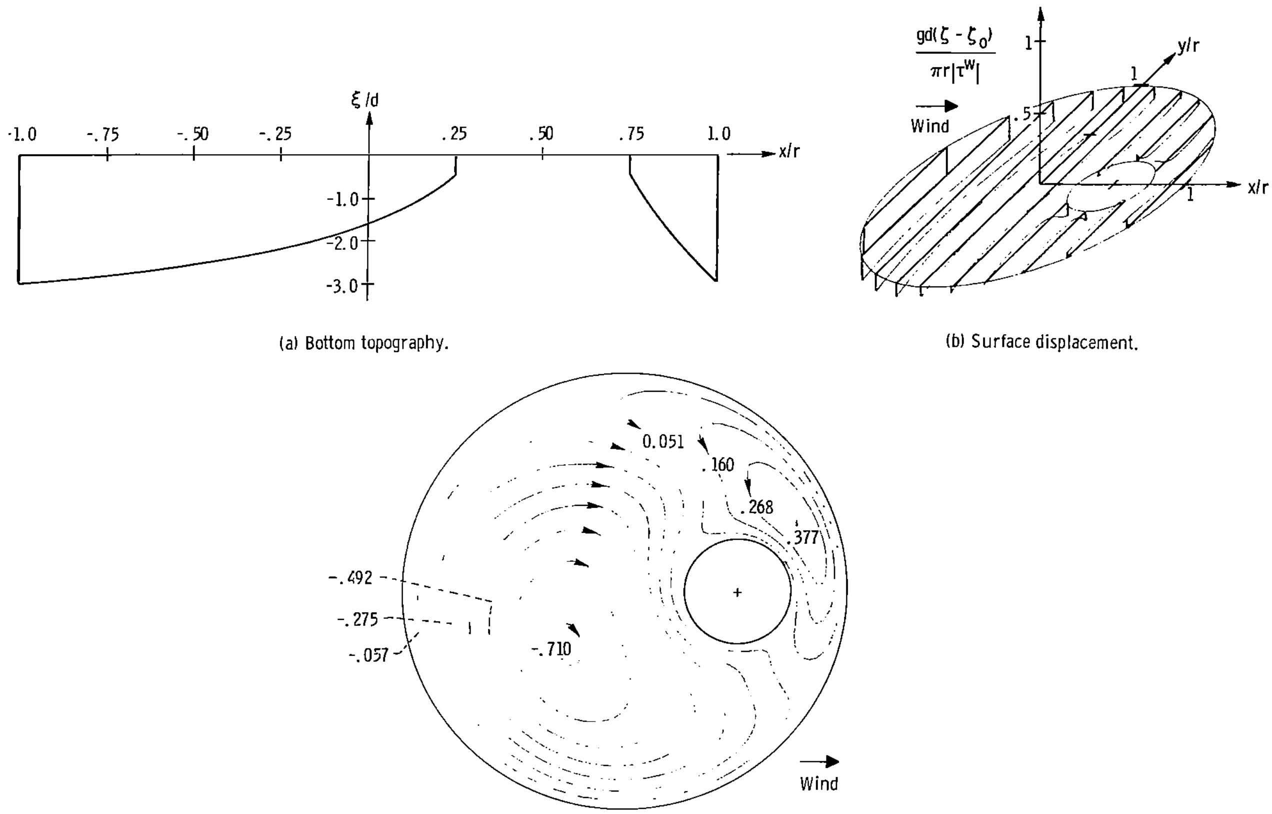

(a) Bottom topography.

(b) Surface displacement.

(c) Nondimensional stream function $2\pi f_c \psi / |\tau^W|$.

Figure 19. - Circular basin circulation. Island eccentricity = 0.5; island diameter = 0.5; h/d = 3.0 at mainland shore; h/d = 0.5 at island; $\tau^W/|\tau^W| = 1.0$.

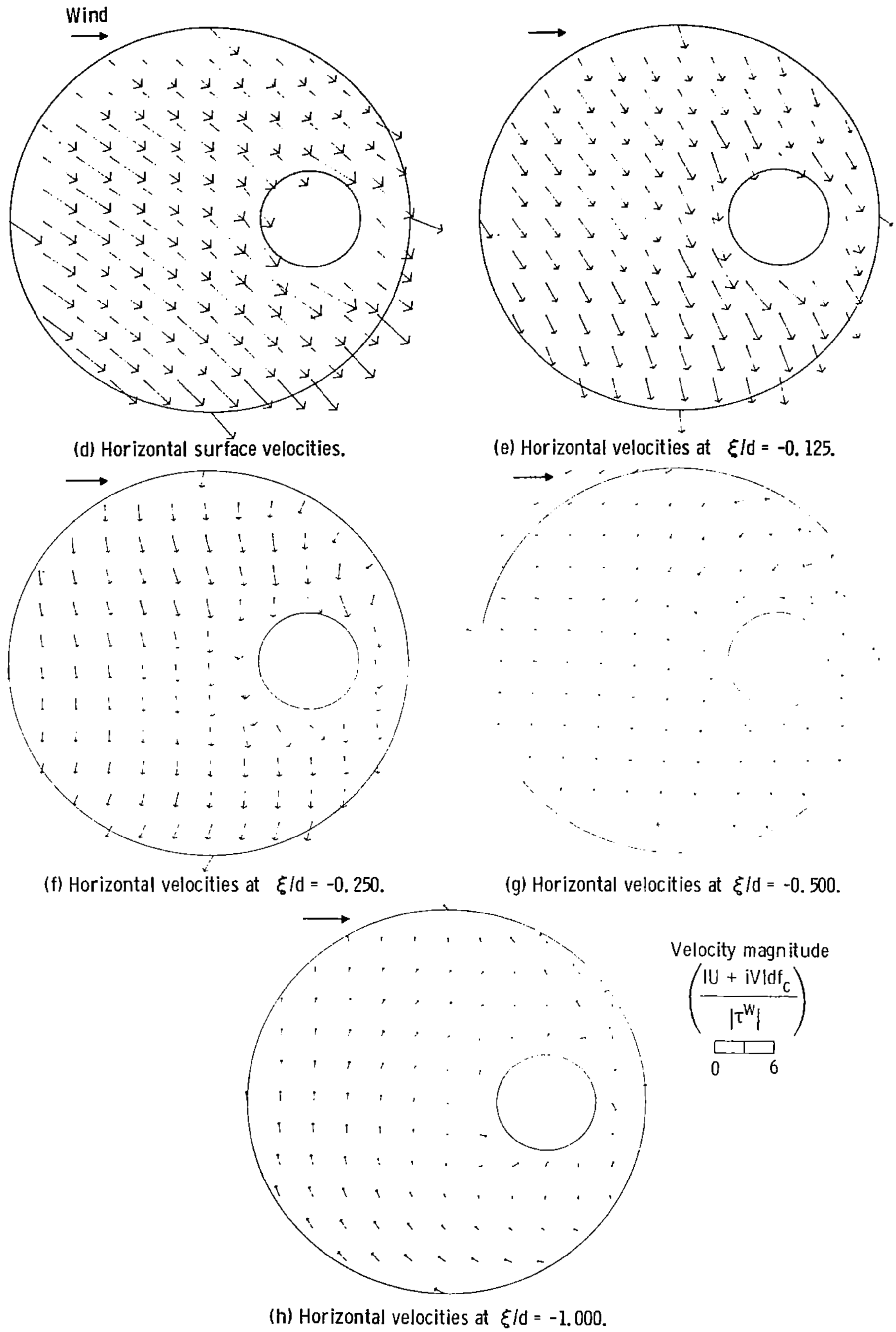

(d) Horizontal surface velocities.

(e) Horizontal velocities at $\xi/d = -0.125$.

(f) Horizontal velocities at $\xi/d = -0.250$.

(g) Horizontal velocities at $\xi/d = -0.500$.

(h) Horizontal velocities at $\xi/d = -1.000$.

Figure 19. - Concluded.

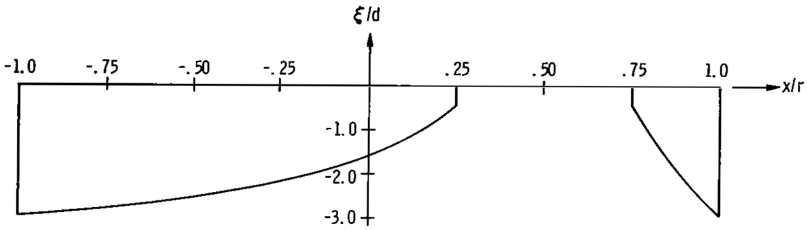

(a) Bottom topography.

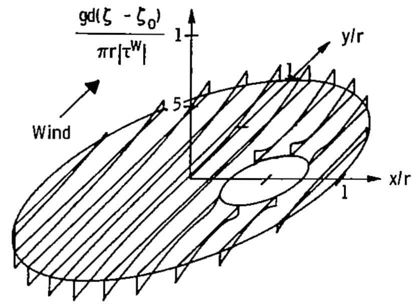

(b) Surface displacement.

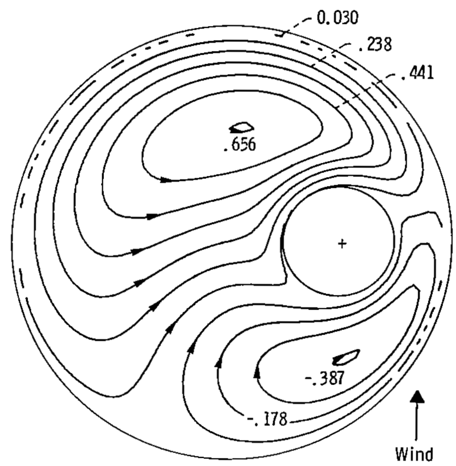

(c) Nondimensional stream function $2\pi f_c \psi / |\tau^W|$.

Figure 20. - Circular basin circulation. Island eccentricity = 0.5; island diameter = 0.5; h/d = 3.0 at mainland shore; h/d = 0.5 at island; $\tau^W/|\tau^W| = i$.

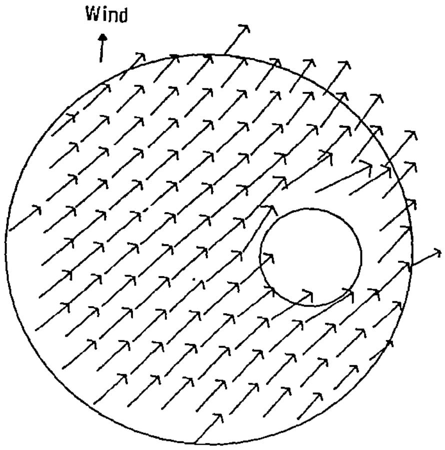

(d) Horizontal surface velocities.

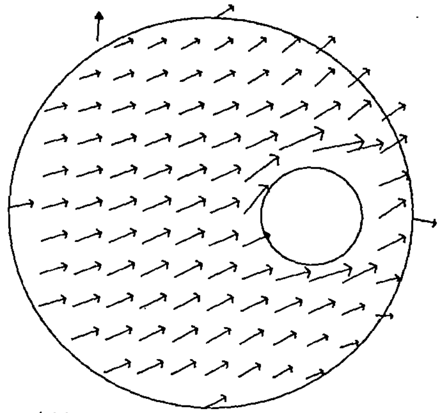

(e) Horizontal velocities at $\xi/d = -0.125$.

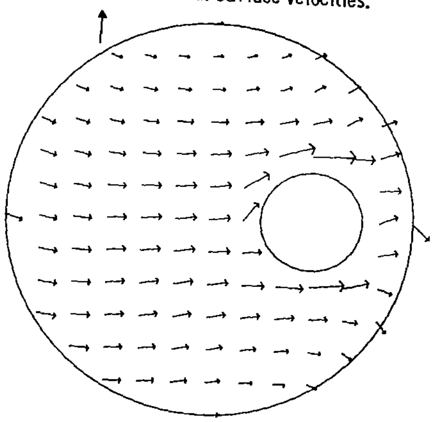

(f) Horizontal velocities at $\xi/d = -0.250$.

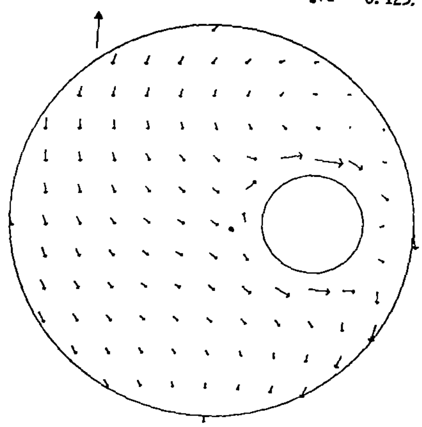

(g) Horizontal velocities at $\xi/d = -0.500$.

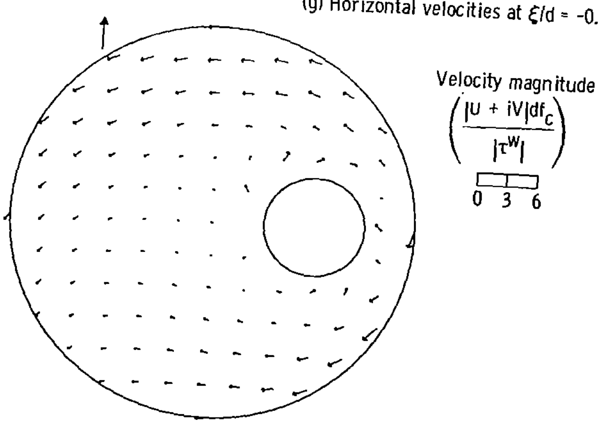

(h) Horizontal velocities at $\xi/d = -1.000$.

Figure 20. - Concluded.

NATIONAL AERONAUTICS AND SPACE ADMISTRATION
WASHINGTON, D.C. 20546

OFFICIAL BUSINESS
PENALTY FOR PRIVATE USE $300

FIRST CLASS MAIL

POSTAGE AND FEES PAID
NATIONAL AERONAUTICS AND
SPACE ADMINISTRATION

U.S.MAIL

017 001 C1 U 13 711029 S00903DS
DEPT OF THE AIR FORCE
AF WEAPONS LAB (AFSC)
TECH LIBRARY/WLOL/
ATTN: E LOU BOWMAN, CHIEF
KIRTLAND AFB NM 87117

POSTMASTER: If Undeliverable (Section 15
Postal Manual) Do Not Ret

"The aeronautical and space activities of the United States shall be conducted so as to contribute . . . to the expansion of human knowledge of phenomena in the atmosphere and space. The Administration shall provide for the widest practicable and appropriate dissemination of information concerning its activities and the results thereof."

—NATIONAL AERONAUTICS AND SPACE ACT OF 1958

NASA SCIENTIFIC AND TECHNICAL PUBLICATIONS

TECHNICAL REPORTS: Scientific and technical information considered important, complete, and a lasting contribution to existing knowledge.

TECHNICAL NOTES: Information less broad in scope but nevertheless of importance as a contribution to existing knowledge.

TECHNICAL MEMORANDUMS: Information receiving limited distribution because of preliminary data, security classification, or other reasons.

CONTRACTOR REPORTS: Scientific and technical information generated under a NASA contract or grant and considered an important contribution to existing knowledge.

TECHNICAL TRANSLATIONS: Information published in a foreign language considered to merit NASA distribution in English.

SPECIAL PUBLICATIONS: Information derived from or of value to NASA activities. Publications include conference proceedings, monographs, data compilations, handbooks, sourcebooks, and special bibliographies.

TECHNOLOGY UTILIZATION PUBLICATIONS: Information on technology used by NASA that may be of particular interest in commercial and other non-aerospace applications. Publications include Tech Briefs, Technology Utilization Reports and Technology Surveys.

Details on the availability of these publications may be obtained from:

SCIENTIFIC AND TECHNICAL INFORMATION OFFICE

NATIONAL AERONAUTICS AND SPACE ADMINISTRATION

Washington, D.C. 20546